

Joint Antenna and Relay Selection Strategies for Decode-and-Forward Relay Networks

Swaminathan R, *Student Member, IEEE*, George K. Karagiannidis, *Fellow, IEEE*, and Rajarshi Roy, *Member, IEEE*

Abstract—Cooperative diversity systems with optimal and suboptimal antenna and relay selection have been paid significant attention for more than half a decade. However, optimal antenna and relay selection strategies require global channel state information (CSI), which is a cumbersome process. In this paper, we propose a diversity-optimal and three suboptimal transmit–receive antenna and relay selection strategies, named S1, S2, and S3, for decode-and-forward cooperative relaying systems, equipped with N_t and N_r antennas at the source (S) and the destination (D), respectively, and considering a multirelay scenario. Furthermore, we study the symbol error probability (SEP) for these strategies, assuming M -ary phase-shift keying signaling over Rayleigh fading channels. In addition, we perform diversity order analysis through closed-form asymptotic SEP expressions. Since the proposed suboptimal strategies, i.e., S2 and S3, involve the so-called switch-and-examine combining scheme, we compare the complexity of S1, S2, and S3 in terms of the average number of CSI required at D to select the best transmit–receive antenna pair and relay. From the derived SEP expressions, it can be concluded that all three suboptimal strategies achieve the same diversity order of $N_t N_r + N$, where N is the number of relays, except for the case when the switching threshold signal-to-noise ratio (SNR) is much lower than the average SNR in S2 and S3. Finally, the diversity-optimal strategy achieves full diversity order of $N_t N_r + N \min(N_t, N_r)$.

Index Terms—Antenna and relay selection strategies, decode-and-forward (DF), M -ary phase-shift keying (MPSK), Rayleigh fading, switch-and-examine combining (SEC), symbol error probability (SEP).

I. INTRODUCTION

COOPERATIVE communications have emerged as a potential candidate for achieving improved error performance due to distributed spatial diversity gain. Amplify-and-forward (AF) and decode-and-forward (DF) are the two prominent relaying protocols, whereby the source (S) can transmit to the destination (D) through randomly distributed relay nodes. The performance of single-input–single-output DF-relaying-based

cooperative diversity systems has been extensively investigated in the literature [1]–[8]. Owing to ease of implementation, most of the work on performance analysis is focused on the DF relaying system. Specifically, in [1]–[3], the symbol error probability (SEP) of a cooperative diversity system equipped with a single DF relay was studied over Rayleigh fading channels, whereas in [4]–[6], various DF selection strategies were analyzed. More specifically, in [2]–[6], it was observed that full diversity order can be achieved only if the channel state information (CSI) of all links is available at the destination. However, in the case of a multirelay scenario, the estimation of CSI of all the links is a high-complexity process. Therefore, distributed switched diversity combining schemes, such as switch-and-stay combining and switch-and-examine combining (SEC) schemes, which require less CSI at D, have been proposed for cooperative diversity systems in [7] and [8], respectively.

For more than a decade, the cooperative multiple-input multiple-output (MIMO) system has acquired significant attention. In [9]–[11], the performance of the DF relaying MIMO system with beamforming and orthogonal space–time block code (OSTBC) techniques was studied. However, these techniques increase the system complexity, since more than one radio frequency chain or antenna should be active for the OSTBC technique, and both amplitude and phase information of the channels is required at the transmitter for the beamforming technique. Therefore, to reduce the complexity, antenna selection strategies were proposed. The performance analysis of antenna and relay selection strategies is being actively investigated for cooperative diversity systems, and various suboptimal and optimal antenna and relay selection strategies were proposed in [12]–[17]. In [12], approximate SEP and outage probability expressions were derived for suboptimal and optimal transmit antenna selection (TAS) strategies that were considering a cooperative MIMO system with a single AF relay. The optimal TAS selects the transmit antenna, which maximizes the postprocessing signal-to-noise ratio (SNR) at D, and this D requires the CSI of all links. In the case of suboptimal TAS, based on the CSI of source-to-destination (SD) and relay-to-destination (RD) links, best transmit antennas for S and relay nodes are selected, respectively.

In [13] and [14], the performance of joint relay and antenna selection strategies for dual-hop multirelay AF and DF relaying MIMO systems, respectively, was studied through SEP and outage probability expressions. In [15], a multirelay DF relaying MIMO system with a direct SD link was considered. However, only the TAS strategy at S was proposed without receive antenna and relay selection. Furthermore, two suboptimal antenna selection strategies were proposed in [16] for a single-relay

Manuscript received January 21, 2015; revised June 26, 2015 and October 2, 2015; accepted December 1, 2015. Date of publication January 6, 2016; date of current version November 10, 2016. The review of this paper was coordinated by Dr. L. Zhao.

Swaminathan R is with the School of Computer Engineering, Nanyang Technological University, Singapore 639798 (e-mail: swaminathan.ramabadrana@gmail.com).

G. K. Karagiannidis is with the Provincial Key Lab of Information Coding and Transmission, Southwest Jiaotong University, Chengdu 610031, China, and also with the Electrical and Computer Engineering Department, Aristotle University of Thessaloniki, 541 24 Thessaloniki, Greece (e-mail: geokarag@auth.gr).

R. Roy is with the Department of Electronics and Electrical Communication Engineering, Indian Institute of Technology (IIT) Kharagpur, Kharagpur 721 302, India (e-mail: royr@ece.iitkgp.ernet.in).

Digital Object Identifier 10.1109/TVT.2016.2515265

cooperative MIMO system, and upper bounds on SEP were derived over Rayleigh fading channels. More recently, in [17], a joint antenna and path selection technique for the single-DF-relay cooperative MIMO system was proposed. It was observed that the proposed technique is diversity optimal and achieves full diversity order. Here, the path selection was performed first, and after that, based on the maximum instantaneous SNR values of SD, source-to-relay (SR), and RD links, the transmit–receive antenna pair was selected. Furthermore, the switched-diversity-combining-based transmit–receive antenna selection strategy was proposed in [18] for a MIMO scenario, and the performance was studied over Rayleigh fading channels.

A. Motivation

The main motivation of this paper can be summarized as follows.

- The literature lacks in the SEP analysis of optimal and suboptimal antenna and relay selection strategies for the DF system with a direct SD link, which considers a multirelay scenario. Furthermore, most of the works in the multirelay scenario are limited to AF and dual-hop DF MIMO systems without a direct SD link.
- The optimal antenna and relay selection strategies proposed for the AF and DF relaying systems require CSI knowledge of all the links at D. Therefore, there is a need to examine the performance of suboptimal antenna and relay selection strategies.
- The performance analysis of the SEC-based antenna selection strategy is limited to MIMO systems. However, to the best of our knowledge, SEC-based antenna selection strategies have not been explored for a cooperative diversity scenario.

B. Contribution

The main contribution of this paper is as follows.

- The average end-to-end SEP expressions are derived for three different suboptimal antenna and relay selection strategies that consider a DF multirelay system with a direct SD link over slow, flat, and independent Rayleigh fading channels, which assume M -ary phase-shift keying (MPSK) signaling.
- For the sake of comparison, a closed-form, upper bound expression for the average SEP of a diversity-optimal strategy is derived, instead of a complex exact expression.
- Closed-form asymptotic SEP expressions are derived for the proposed strategies to evaluate the diversity order.
- A complexity comparison of all the proposed strategies in terms of the average number of CSI required at D is performed by means of Monte Carlo simulations.

C. Benefits of the Proposed Strategies

- The suboptimal antenna selection strategies require less communication overhead compared with the diversity-optimal antenna selection strategy proposed in our work

as well as that in [17], since the CSI of SR and RD links is not required in selecting the best antenna pair.

- The proposed suboptimal strategies select the best antenna pair from the instantaneous SNR values of $N_t N_r$ SD links, where N_t and N_r denote the number of transmit and receive antennas at S and D, respectively. However, there could be other possible ways of selecting the best antenna pair. Similar to [16], the source antenna could be selected based on the best SD or SR links, and the destination antenna could be selected based on the best RD links. If the antenna pair is selected based on the best SD and RD links, then the instantaneous SNR values of $N_t N_r$ SD links and $N N_r$ RD links are required (i.e., total $N_t N_r + N N_r$ links), where N is the number of relays. In addition, if the same is selected based on the best SR and RD links, then the instantaneous SNR values of $N N_t$ SR links and $N N_r$ RD links are required.
- Hence, the antenna selection strategies proposed in our work based on SD links alone require less CSI to select the antenna pair compared with both strategies proposed in [16], however, at the expense of performance degradation.
- As two of the proposed strategies employ the SEC scheme, the number of channel estimations is considerably reduced in comparison with other proposed schemes in the literature.

D. Structure and Notations

The rest of this paper is organized as follows. The system model of a multirelay cooperative diversity system considering multiple antennas at S and D is given in Section II. In Section III, diversity-optimal and three suboptimal strategies are discussed. The average and asymptotic SEPs of all the proposed strategies are derived over Rayleigh fading channels in Section IV. The impact of outdated/delayed CSI is discussed in Section V, followed by numerical results and discussions in Section VI. Finally, the concluding remarks are given in Section VII.

Let us denote strategies I, II, and III as S1, S2, and S3, respectively, for convenience. Moreover, unless otherwise mentioned, $(\cdot)^*$ and $|\cdot|$ denote the complex conjugate and absolute value operations, respectively, and $\Gamma(\cdot)$ indicates the gamma integral function. Moreover, $\gamma(\cdot, \cdot)$ and $\Gamma(\cdot, \cdot)$ denote the lower and upper incomplete gamma functions, respectively.

II. SYSTEM MODEL

We consider a communication network consisting of a source (S_i), employed with N_t transmit antennas, where $i = 1, 2, \dots, N_t$, N single-antenna DF relay (R_j) nodes, where $j = 1, 2, \dots, N$, and a single destination node (D_b) with N_r receive antennas, where $b = 1, 2, \dots, N_r$, with the presence of the direct SD link, as shown in Fig. 1. A practical scenario of the model under consideration could be a mobile node (S_i), which communicates with the base station (D_b), with the help of other randomly distributed mobile nodes (R_j). We assume symbol-by-symbol transmission, where, in the first phase, the selected k th transmit antenna broadcasts the baseband information

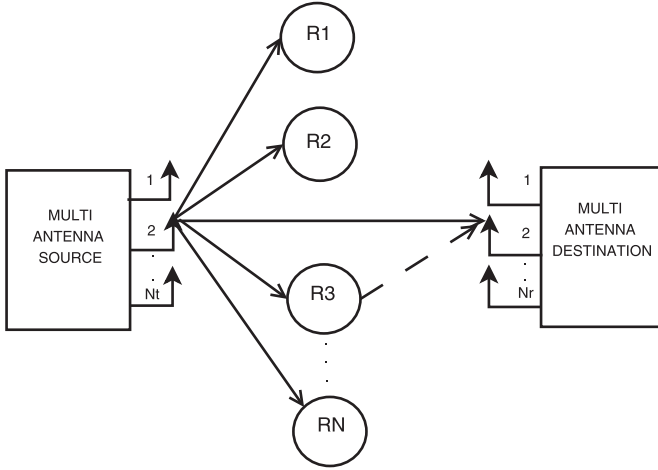


Fig. 1. Multi-DF-relay system with single-antenna relay nodes and multiple antennas at the source and destination nodes.

symbol s to all the relay nodes and D. The symbol s belongs to an MPSK constellation with energy $2E_s$ in the signal space S' (i.e., $S' = \{S'_1, \dots, S'_M\}, s \in S'$), where $S'_n = \sqrt{2E_s} \times \exp(-j2\pi(n-1)/M), n=1, \dots, M, j = \sqrt{-1}$. Let us assume that the c th receive antenna is selected at D. The received complex baseband information symbols at R_j and D_c are, respectively, given by

$$r_{S_k R_j} = h_{S_k R_j} s + n_{S_k R_j} \quad (1)$$

$$r_{S_k D_c} = h_{S_k D_c} s + n_{S_k D_c} \quad (2)$$

where $h_{S_k R_j}$ and $h_{S_k D_c}$ indicate the fading channel coefficients between S_k and R_j and between S_k and D_c , respectively, and $n_{S_k R_j}$ and $n_{S_k D_c}$ represent the additive white Gaussian noise (AWGN) at R_j and D_c , respectively. The decision rule for detecting the received baseband information symbol at R_j is given by

$$\hat{s}_j = \arg \left\{ \max_{s \in S'} \operatorname{Re} (s^* h_{S_k R_j}^* r_{S_k R_j}) \right\}. \quad (3)$$

It is assumed that $h_{S_k R_j}$ is known at R_j . In phase II, the selected relay R_l forwards the detected symbol \hat{s}_l to D. The received complex baseband information symbol at D_c is given by

$$r_{R_l D_c} = h_{R_l D_c} \hat{s}_l + n_{R_l D_c} \quad (4)$$

where $h_{R_l D_c}$ indicates the fading channel coefficient between R_l and D_c , and $n_{R_l D_c}$ represents the AWGN at D_c . All the fading channel coefficients above are modeled as zero-mean complex Gaussian random variables (RVs), and so, their absolute values follow Rayleigh distribution. Moreover, the AWGN noise is modeled as a complex Gaussian RV with zero mean and variance of $2N_0$.

Let us define γ_{SD} , γ_{SR_l} , and $\gamma_{R_l D}$ as the instantaneous SNR values of SD, l th SR, and l th RD links, respectively, which are given by $\gamma_{SD} = (E_s/N_0)|h_{SD}|^2$, $\gamma_{SR_l} = (E_s/N_0)|h_{SR_l}|^2$, and $\gamma_{R_l D} = (E_s/N_0)|h_{R_l D}|^2$. Furthermore, since $|h_{SD}|$, $|h_{SR_l}|$, and $|h_{R_l D}|$ follow a Rayleigh distribution, $|h_{SD}|^2$, $|h_{SR_l}|^2$, and $|h_{R_l D}|^2$ follow an exponential distribution. Therefore, the instantaneous SNR of SD, l th SR, and l th RD links also follow an exponential distribution with mean equal to their corresponding average SNR values, which are denoted by $\bar{\gamma}_{SD}$, $\bar{\gamma}_{SR_l}$,

and $\bar{\gamma}_{R_l D}$, respectively. Finally, it is assumed that the CSI of SR, SD, and RD links remains almost constant during the two phases of symbol transmission.

III. ANTENNA AND RELAY SELECTION STRATEGIES

A. Diversity-Optimal Strategy

The following are the steps involved in selecting the best antenna pair and relay.

- *Step 1:* First, the maximum instantaneous SNR values of SD, RD, and SR links are evaluated. After that, the SD link (i.e., direct path) or the source-to-relay-to-destination (SRD) link (i.e., cooperative path) is selected based on the following decision rule:

$$\gamma_{\text{sel}} = \max \left(\gamma_{S_k D_c}, \min_{j \in \{1, \dots, N\}} (\gamma_{S_k R_j}, \gamma_{R_j D_c}) \right). \quad (5)$$

- *Step 2:* If the SD link is chosen, the transmit–receive antenna pair is selected based on the instantaneous SNR values of the best SD links and is given by

$$\{k, c\} = \arg \max_{\substack{1 \leq i \leq N_t, \\ 1 \leq b \leq N_r}} (\gamma_{S_i D_b}). \quad (6)$$

- *Step 3:* If the l th SRD link is chosen, then the k th source antenna and the c th destination antenna are selected based on the instantaneous SNR values of the best l th SR and RD links, respectively, and are given by

$$\begin{aligned} \{k\} &= \arg \max_{1 \leq i \leq N_t} (\gamma_{S_i R_l}) \\ \{c\} &= \arg \max_{1 \leq b \leq N_r} (\gamma_{R_l D_b}). \end{aligned} \quad (7)$$

The proposed antenna and relay selection strategy is similar to the path and antenna selection strategy discussed in [17]. However, as already mentioned, the work in [17] is restricted to the single-relay cooperative MIMO system. Moreover, the proposed strategy in our work is not SNR optimal as selection combining (SC) is employed in combining SD and SRD links. However, it is diversity optimal since it achieves full diversity order of $N_t N_r + N \min(N_t, N_r)$ similar to the optimal scheme proposed in [15] for a multirelay cooperative MIMO system.

B. Suboptimal Strategy I

- *Step 1:* In suboptimal strategy I (S1), we choose the transmit–receive antenna pair based on the instantaneous SNR values of the best SD links as follows:

$$\{k, c\} = \arg \max_{\substack{1 \leq i \leq N_t, \\ 1 \leq b \leq N_r}} (\gamma_{S_i D_b}). \quad (8)$$

- *Step 2:* After choosing the antenna pair, the best relay in the cooperative path or the direct path is selected based on the following decision rule:

$$\gamma_{\text{sel}} = \max \left(\gamma_{S_k D_c}, \min_{j \in \{1, \dots, N\}} (\gamma_{S_k R_j}, \gamma_{R_j D_c}) \right). \quad (9)$$

Since the transmit–receive antenna pair for the direct and cooperative paths is chosen based on the instantaneous SNR values of the best SD links alone, the scheme is suboptimal.

C. Suboptimal Strategy II

In suboptimal strategy II (S2), the antenna selection decision rule remains the same as that of S1 and is given by (8). The following are the steps involved in S2 for selecting the antenna pair and relay.

- *Step 1:* In the guard period before each transmission phase, S from each transmit antenna sends ready-to-send (RTS) packets to D.
- *Step 2:* From the received RTS packets, D estimates the CSI of all SD links and evaluates the instantaneous SNR values. Then, the transmit–receive antenna pair is selected based on (8).
- *Step 3:* If $\gamma_{S_k D_c} > \gamma_t$, where γ_t denotes the switching threshold SNR value, D sends a positive acknowledgement (ACK) to S to start the transmission phase along with the information of the selected transmit antenna.
- *Step 4:* S from the k th transmit antenna sends a positive flag message to all the relay nodes. After receiving the same from S_k , all the relays will enter into idle mode during that particular transmission. The baseband information symbol is transmitted from S_k , and the received signal at D_c is given by (2).
- *Step 5:* If $\gamma_{S_k D_c} < \gamma_t$, then D sends a negative ACK to S along with the information of the selected transmit antenna.
- *Step 6:* S_k broadcasts an RTS packet to all the relay nodes. After receiving the packet, all the relay nodes start a timer.
- *Step 7:* Let us assume that the timer of the l th relay node gets expired first. Then, R_l updates the value of counter $l = l + 1$. If $l \neq N$, then R_l estimates the CSI of the SR link (i.e., $h_{S_k R_l}$) and transmits the estimate along with the RTS packet to D. By overhearing the RTS packet from another relay node, all the other relay nodes update the value of counter $l = l + 1$ without sending anything and will go into listening mode.
- *Step 8:* After receiving the RTS packet, D estimates the CSI of the RD link at the c th receive antenna and evaluates $\gamma_l = \min(\gamma_{S_k R_l}, \gamma_{R_l D_c})$.
- *Step 9:* If $\gamma_l > \gamma_t$, then D sends a positive ACK to the l th relay node to decode and forward the signal received from S in the second orthogonal phase of transmission. Moreover, the l th relay node sends a positive flag message to all the other relay nodes and S. After receiving the flag message from the l th relay node, S will start the transmission phase, and the other relay nodes, which are in the listening mode, will enter into idle mode. During the first and second phases of the transmission, the received signals at the relay node and D in the cooperative path are, respectively, given by (1) and (4).
- *Step 10:* If $\gamma_l < \gamma_t$, the l th relay node will be negatively acknowledged by D. Then, the l th relay node sends a negative flag message to all the other relay nodes to start

their timer. The relay node whose timer gets expired next will continue the same process as already mentioned in Steps 7–9.

- *Step 11:* If $l = N$ in Step 7, it implies that both direct and $N - 1$ cooperative paths fail to satisfy the threshold SNR condition. Hence, the last relay node, without estimating the CSI of the SR link, sends a positive flag message to all the other relay nodes and S. After receiving the flag message from the l th relay node, S will start the transmission phase. Hence, the last cooperative path is selected without being examined.

D. Suboptimal Strategy III

In suboptimal strategy III (S3), both antenna and relay selection will be performed with the help of the SEC scheme. The possible transmit–receive antenna pair is given by

$$\{k, c\} = [\{1, 1\}, \dots, \{1, N_r\}, \dots, \{N_t, 1\}, \dots, \{N_t, N_r\}].$$

The following are the steps involved in S3 for selecting the antenna pair and relay.

- *Step 1:* Here, S sends an RTS packet from the first antenna to D. From the received packet, if $\gamma_{S_1 D_1} > \gamma_t$, then $\{k, c\} = [\{1, 1\}]$; else, $\gamma_{S_1 D_2}$ will be evaluated. Likewise, the transmit–receive antenna selection process will continue similar to the SEC scheme until $\{k, c\} = [\{N_t, N_r - 1\}]$. If $\gamma_{S_{N_t} D_{N_r - 1}} < \gamma_t$, then $\{k, c\} = [\{N_t, N_r\}]$. After selecting the antenna pair, D sends the information related to the selected transmit antenna.
- *Step 2:* See Steps 6–8 in Section III-C.
- *Step 3:* If $\gamma_l > \gamma_t$, then D sends a positive ACK to the l th relay node. Moreover, the l th relay node sends a positive flag message to all the other relay nodes. After receiving the flag message, all other relay nodes, which are in the listening mode, will enter into idle mode.
- *Step 4:* If $\gamma_l < \gamma_t$, the l th relay node will be negatively acknowledged by D. Then, the l th relay node sends a negative flag message to all the other relay nodes to start their timer. The relay node whose timer gets expired next will continue the same process as already mentioned in Steps 2 and 3.
- *Step 5:* After selecting the cooperative path (assuming that the l th relay node is chosen), it is compared with the direct path according to the decision rule $\max(\gamma_{S_k D_c}, \min(\gamma_{S_k R_l}, \gamma_{R_l D_c}))$. Note that if the threshold SNR condition is not satisfied for $N_t N_r - 1$ direct and $N - 1$ cooperative paths, then $l = N$, and $\{k, c\} = [\{N_t, N_r\}]$.
- *Step 6:* Finally, after selecting the cooperative or the direct path, D asks S to start the transmission phase.

Note that S2 does not compare the direct path with the cooperative path similar to S3 according to the decision rule given in Step 5. If $\gamma_{S_k D_c} > \gamma_t$, then S2 neglects the cooperative path. However, in S3, although $\gamma_{S_k D_c} > \gamma_t$, it compares the direct path with the best cooperative path for the transmission. Moreover, it seems that choosing the best antenna pair and relay by comparing them with γ_t could take time to work in S2 and S3

when compared with the optimal strategy. However, the delay in examining a particular path is compensated by the number of channel estimations required to select the best antenna pair and relay, as the delay is considerably reduced in S2 and S3 compared with the diversity-optimal strategy and S1. The SEC scheme in S2 and S3 can be implemented in a centralized manner, and D acts as a centralized node in communicating the selected relay node and transmit antenna index back to the transmitting nodes and fixing the threshold SNR value before examining the links.

E. Probability Density Function and Cumulative Density Function

Since the instantaneous SNR of the SD, SR, and RD links follow an exponential distribution, the corresponding probability density function (pdf) and cumulative distribution function (cdf) are given by

$$f_{\gamma_{ii}}(t) = \frac{1}{\bar{\gamma}_{ii}} \exp\left(\frac{-t}{\bar{\gamma}_{ii}}\right), F_{\gamma_{ii}}(t) = 1 - \exp\left(\frac{-t}{\bar{\gamma}_{ii}}\right) \quad (10)$$

where $ii \in \{\text{SR}_l, R_l D, \text{SD}\}$. Let $\delta_{\text{SR}} = \max(S_1 R_l, \dots, S_{N_t} R_l)$, $\delta_{\text{RD}} = \max(R_l D_1, \dots, R_l D_{N_r})$, and $\delta_{\text{SD}} = \max(S_1 D_1, \dots, S_{N_t} D_{N_r})$ represent the maximum instantaneous SNR values of the l th SR, l th RD, and SD links, respectively. The cdf of δ_{ii} , where $ii \in \{\text{SR}, \text{RD}, \text{SD}\}$, for the SR, RD, and SD links are, respectively, given by

$$\begin{aligned} F_{\delta_{\text{SR}}}(t) &= \left\{ 1 - \exp\left(\frac{-t}{\bar{\gamma}_{\text{SR}}}\right) \right\}^{N_t} \\ F_{\delta_{\text{RD}}}(t) &= \left\{ 1 - \exp\left(\frac{-t}{\bar{\gamma}_{\text{RD}}}\right) \right\}^{N_r} \\ F_{\delta_{\text{SD}}}(t) &= \left\{ 1 - \exp\left(\frac{-t}{\bar{\gamma}_{\text{SD}}}\right) \right\}^{N_t N_r}. \end{aligned} \quad (11)$$

Furthermore, the pdf of δ_{ii} for the SR, RD, and SD links are, respectively, given by

$$\begin{aligned} f_{\delta_{\text{SR}}}(t) &= \frac{N_t \exp\left(\frac{-t}{\bar{\gamma}_{\text{SR}}}\right)}{\bar{\gamma}_{\text{SR}}} \left\{ 1 - \exp\left(\frac{-t}{\bar{\gamma}_{\text{SR}}}\right) \right\}^{N_t-1} \\ f_{\delta_{\text{RD}}}(t) &= \frac{N_r \exp\left(\frac{-t}{\bar{\gamma}_{\text{RD}}}\right)}{\bar{\gamma}_{\text{RD}}} \left\{ 1 - \exp\left(\frac{-t}{\bar{\gamma}_{\text{RD}}}\right) \right\}^{N_r-1} \\ f_{\delta_{\text{SD}}}(t) &= \frac{N_r N_t \exp\left(\frac{-t}{\bar{\gamma}_{\text{SD}}}\right)}{\bar{\gamma}_{\text{SD}}} \left\{ 1 - \exp\left(\frac{-t}{\bar{\gamma}_{\text{SD}}}\right) \right\}^{N_r N_t-1}. \end{aligned} \quad (12)$$

Let us define an RV V_j , which is given by $V_j = \min(\gamma_{\text{SR}_j}, \gamma_{R_j D})$, and the corresponding cdf can be expressed as

$$F_{V_j}(t) = 1 - \int_t^{\infty} \int_t^{\infty} f_{\gamma_{\text{SR}_j}}(t_3) f_{\gamma_{R_j D}}(t_2) dt_2 dt_3 = 1 - \exp(-A_j t) \quad (13)$$

where $A_j = (1/\bar{\gamma}_{\text{SR}_j}) + (1/\bar{\gamma}_{R_j D})$. Let us define another RV δ , which is given by $\delta = \min(\delta_{\text{SR}}, \delta_{\text{RD}})$, and the corresponding cdf can be expressed as [17, eq. (6)]

$$F_{\delta}(t) = F_{\delta_{\text{SR}}}(t) + F_{\delta_{\text{RD}}}(t) - F_{\delta_{\text{SR}}}(t)F_{\delta_{\text{RD}}}(t). \quad (14)$$

Differentiating (13), the pdf of V_j can be expressed as

$$f_{V_j}(t) = A_j \exp(-A_j t). \quad (15)$$

Similarly, differentiating (14), the pdf of δ can be expressed as [17, eq. (6)]

$$f_{\delta}(t) = f_{\delta_{\text{SR}}}(t) (1 - F_{\delta_{\text{RD}}}(t)) + f_{\delta_{\text{RD}}}(t) (1 - F_{\delta_{\text{SR}}}(t)). \quad (16)$$

IV. PERFORMANCE ANALYSIS

A. Diversity-Optimal Strategy

An upper bound on the conditional SEP of MPSK signaling conditioned on the instantaneous SNR of any given link γ is given by [19, eq. (8.24)]

$$P_e(\gamma) \leq \frac{M-1}{M} \exp\left(-\gamma \sin^2\left(\frac{\pi}{M}\right)\right). \quad (17)$$

Note that the end-to-end SEP is obtained by assuming $\bar{\gamma}_{\text{SR}} = \bar{\gamma}_{S_i R_j}$, $\bar{\gamma}_{\text{RD}} = \bar{\gamma}_{R_j D_b}$, and $\bar{\gamma}_{\text{SD}} = \bar{\gamma}_{S_i D_b}$. The average SEP of the direct SD link based on the decision rule given by (5) can be expressed as

$$P_{e\text{SD}}^{\text{opt}} = \int_0^{\infty} P_e(t_1) f_{\delta_{\text{SD}}}(t_1) (F_{\delta}(t_1))^N dt_1. \quad (18)$$

Substituting (12), (14), and (17) in (18), the upper bound on (18) in closed form is given by

$$\begin{aligned} P_{e\text{SD}}^{\text{opt}} &\leq \frac{N_t N_r (M-1)}{M \bar{\gamma}_{\text{SD}}} \sum_{m=0}^{N_t N_r - 1} \binom{N_t N_r - 1}{m} (-1)^m \\ &\times \left\{ \sum_{n=0}^{N_t N} \binom{N_t N}{n} \frac{(-1)^n}{\sin^2\left(\frac{\pi}{M}\right) + \frac{m+1}{\bar{\gamma}_{\text{SD}}} + \frac{n}{\bar{\gamma}_{\text{SR}}}} \right. \\ &\left. + \sum_{p=0}^{N_r N} \binom{N_r N}{p} \frac{(-1)^p}{\sin^2\left(\frac{\pi}{M}\right) + \frac{m+1}{\bar{\gamma}_{\text{SD}}} + \frac{p}{\bar{\gamma}_{\text{RD}}}} \right\}. \end{aligned} \quad (19)$$

The conditional error probability of the SRD link [1, eq. (21)] is then expressed as¹

$$P_{e\text{SRD}}(\gamma_{\text{SR}}, \gamma_{\text{RD}}) = P_e(\gamma_{\text{SR}}) + P_e(\gamma_{\text{RD}}) - P_e(\gamma_{\text{SR}})P_e(\gamma_{\text{RD}}). \quad (20)$$

The average SEP of the SRD link based on the decision rule given by (5) can be expressed as (21), shown at the bottom of the next page. Equation (21) is divided into four smaller terms. After substituting (11), (12), (14), and (20) in (21), the upper bounds on $A_1(\cdot, \cdot)$ and $A_2(\cdot, \cdot)$ in closed form after simplification are given by (81a) and (82a), respectively, in

¹Note that the final term in [1, eq. (21)] is omitted, since it will not add any significant change in the end-to-end average SEP, and our simulation results exactly agree with the computed SEP values as well.

the Appendix. The upper bound on the end-to-end SEP of the diversity-optimal strategy by adding the individual SEPs of the SD and SRD links is given by

$$P_e^{\text{opt}} \leq P_{e\text{SD}}^{\text{opt}} + P_{e\text{SRD}}^{\text{opt}}. \quad (22)$$

From (22), we derive the closed-form asymptotic SEP expression by applying high-SNR approximations such as $1 - \exp(-t_1/\bar{\gamma}_{ii}) \approx (t_1/\bar{\gamma}_{ii})$, and $\sin^2(\pi/M) + (1/\bar{\gamma}_{ii}) \approx \sin^2(\pi/M)$. After simplification, the asymptotic SEP of the diversity-optimal strategy that skips detailed derivation steps is given by

$$P_e^{\text{asy}} = \frac{N_t N_r (M-1)}{M} \times \left\{ \frac{\Gamma(N_t N_r + N_t N)}{\{\sin^2(\frac{\pi}{M})\bar{\gamma}\}^{N_t N_r + N_t N}} + \frac{\Gamma(N_t N_r + N_r N)}{\{\sin^2(\frac{\pi}{M})\bar{\gamma}\}^{N_t N_r + N_r N}} \right\} + O\left(\frac{1}{\bar{\gamma}^{N_t N_r + N_r + N_t N}}\right) + O\left(\frac{1}{\bar{\gamma}^{N_t N_r + N_t + N_r N}}\right) \quad (23)$$

where $f(x) = O(g(x))$ if $\lim_{x \rightarrow 0} f(x)/g(x) = 0$. By neglecting the least significant higher-order terms, from (23), it is inferred that the diversity order is equal to $N_t N_r + N \min(N_t, N_r)$.

B. S1

The conditional SEP of MPSK signaling conditioned on γ is given by [19, eq. (8.22)]

$$P_e(\gamma) = \frac{1}{\pi} \int_0^{\phi_0} \exp(-\chi(\phi)\gamma) d\phi \quad (24)$$

where $\phi_0 = \pi(M-1)/M$, and $\chi(\phi) = \sin^2(\pi/M)/\sin^2(\phi)$. Note that the end-to-end SEP of S1 is obtained by assuming $\bar{\gamma}_{\text{SD}} = \bar{\gamma}_{S_i D_b}$. The average SEP of the SD link can then be obtained by averaging (24) over the pdf of the exponential distribution given by (10) under the condition $\gamma_{S_k D_c} > \max_{j \in 1, \dots, N} (\min(\gamma_{S_k R_j}, \gamma_{R_j D_c}))$, and the average is given by

$$P_{e\text{SD}} = N_t N_r \int_0^\infty P_e(t_1) f_{\gamma_{\text{SD}}}(t_1) (F_{\gamma_{\text{SD}}}(t_1))^{(N_t N_r) - 1} \times \prod_{j=1}^N (F_{V_j}(t_1)) dt_1. \quad (25)$$

Then, we define the following quantities:

$$\begin{aligned} \sum_{n=0}^{N-1} \frac{(-1)^n}{n!} &= \sum_{n=0}^{N-1} \frac{(-1)^n}{n!}, \quad \underbrace{\sum_{\substack{k_1=1 \\ k_1 \neq l}}^N \cdots \sum_{\substack{k_n=1 \\ k_n \neq l}}^N}_{k_1, k_2, \dots, k_n \text{ are all distinct}} \\ \sum_{n=0}^N \frac{(-1)^n}{n!} &= \sum_{n=0}^N \frac{(-1)^n}{n!}, \quad \underbrace{\sum_{k_1=1}^N \cdots \sum_{k_n=1}^N}_{k_1, k_2, \dots, k_n \text{ are all distinct}} \\ \alpha_{p,n} &= \sum_{p=1}^n A_{k_p}. \end{aligned} \quad (26)$$

After substituting (24), (10), and (13) in (25), we expand the term $\prod_{j=1}^N (F_{V_j}(t_1))$ by using [5, eq. (9)]. After solving the integral, the average SEP of the SD link is given by

$$P_{e\text{SD}} = \frac{N_t N_r}{\pi \bar{\gamma}_{\text{SD}}} \sum_{m=0}^{N_t N_r - 1} \sum_{n=0}^m \binom{N_t N_r - 1}{m} \times (-1)^m \int_0^{\phi_0} \{\chi(\phi) + \epsilon(n, m)\}^{-1} d\phi \quad (27)$$

where $\epsilon(n, m) = ((m+1)/\bar{\gamma}_{\text{SD}}) + \alpha_{p,n}$.

The average SEP of the SRD link is obtained by averaging (20) over an exponential distribution of the SR and RD links under the condition $\gamma_{S_k D_c} < \min(\gamma_{S_k R_l}, \gamma_{R_l D_c})$. Hence, the average SEP is given by (28), shown at the bottom of the next page. Let us consider Part-A of (28), which is divided into three smaller terms. The first term is given by

$$I_1(\bar{\gamma}_{\text{SR}_l}, \bar{\gamma}_{\text{RD}}) = \int_0^\infty \int_{t_3}^\infty P_e(t_3) f_{\gamma_{\text{SR}_l}}(t_3) f_{\gamma_{\text{RD}}}(t_2) \times \prod_{\substack{j=1 \\ j \neq l}}^N F_{V_j}(t_3) \int_0^{t_3} f_{\gamma_{\text{SD}}}(t_1) (F_{\gamma_{\text{SD}}}(t_1))^{(N_t N_r) - 1} dt_1 dt_2 dt_3. \quad (29)$$

Substituting (24), (10), and (13) in (29), the obtained expression is expanded by using binomial expansion. After solving the

$$P_{e\text{SRD}}^{\text{opt}} = N \left\{ \underbrace{\int_0^\infty \int_{t_3}^\infty P_{e\text{SRD}}(t_3, t_2) f_{\delta_{\text{SR}}}(t_3) f_{\delta_{\text{RD}}}(t_2) (F_\delta(t_3))^{N-1} F_{\delta_{\text{SD}}}(t_3) dt_2 dt_3}_{\mathbf{A}_1(\bar{\gamma}_{\text{SR}}, \bar{\gamma}_{\text{RD}}) + \mathbf{A}_2(\bar{\gamma}_{\text{SR}}, \bar{\gamma}_{\text{RD}})} + \underbrace{\int_0^\infty \int_{t_2}^\infty P_{e\text{SRD}}(t_3, t_2) f_{\delta_{\text{SR}}}(t_3) f_{\delta_{\text{RD}}}(t_2) (F_\delta(t_2))^{N-1} F_{\delta_{\text{SD}}}(t_2) dt_3 dt_2}_{\mathbf{A}_1(\bar{\gamma}_{\text{RD}}, \bar{\gamma}_{\text{SR}}) + \mathbf{A}_2(\bar{\gamma}_{\text{RD}}, \bar{\gamma}_{\text{SR}})} \right\} \quad (21)$$

integrals, the final expression is given by

$$\begin{aligned}
 I_1(\bar{\gamma}_{SR_l}, \bar{\gamma}_{R_lD}) &= \frac{\frac{1}{\pi} \frac{1}{\bar{\gamma}_{SR_l}} \frac{1}{\bar{\gamma}_{SD}}}{\frac{m+1}{\bar{\gamma}_{SD}}} \sum_{m=0}^{N_t N_r - 1} \sum_{n=0}^{N-1} \binom{N_t N_r - 1}{m} (-1)^m \\
 &\times \int_0^{\phi_0} \left\{ (\chi(\phi) + A_l + \alpha_{p,n})^{-1} - (\chi(\phi) + \zeta(n, m))^{-1} \right\} d\phi
 \end{aligned} \tag{30}$$

where $\zeta(n, m) = A_l + \alpha_{p,n} + ((m + 1)/\bar{\gamma}_{SD})$. The second term of Part-A can be obtained by substituting $P_e(t_2)$ for $P_e(t_3)$ in (29), and the final expression is given by

$$\begin{aligned}
 I_2(\bar{\gamma}_{SR_l}, \bar{\gamma}_{R_lD}) &= \frac{\frac{1}{\pi} \frac{1}{\bar{\gamma}_{SR_l}} \frac{1}{\bar{\gamma}_{SD}} \frac{1}{\bar{\gamma}_{R_lD}}}{\frac{m+1}{\bar{\gamma}_{SD}}} \sum_{m=0}^{N_t N_r - 1} \sum_{n=0}^{N-1} \binom{N_t N_r - 1}{m} (-1)^m \\
 &\times \int_0^{\phi_0} (\chi(\phi, \bar{\gamma}_{R_lD}))^{-1} \left\{ (\chi(\phi) + A_l + \alpha_{p,n})^{-1} \right. \\
 &\quad \left. - (\chi(\phi) + \zeta(n, m))^{-1} \right\} d\phi
 \end{aligned} \tag{31}$$

where $\chi(\phi, \bar{\gamma}_{ii}) = \chi(\phi) + 1/\bar{\gamma}_{ii}$. The third term of Part-A can be obtained by substituting $P_e(t_2) P_e(t_3)$ for $P_e(t_3)$ in (29), and the final expression is given by

$$\begin{aligned}
 I_3(\bar{\gamma}_{SR_l}, \bar{\gamma}_{R_lD}, \phi_1, \phi_2) &= \frac{\frac{1}{\pi} \frac{1}{\bar{\gamma}_{SR_l}} \frac{1}{\bar{\gamma}_{SD}} \frac{1}{\bar{\gamma}_{R_lD}}}{\frac{m+1}{\bar{\gamma}_{SD}}} \sum_{m=0}^{N_t N_r - 1} \sum_{n=0}^{N-1} \binom{N_t N_r - 1}{m} (-1)^m \\
 &\times \int_0^{\phi_0} \int_0^{\phi_0} (\chi(\phi_2, \bar{\gamma}_{R_lD}))^{-1} \\
 &\times \left\{ (\chi(\phi_1, \phi_2) + A_l + \alpha_{p,n})^{-1} \right. \\
 &\quad \left. - (\chi(\phi_1, \phi_2) + \zeta(n, m))^{-1} \right\} d\phi_1 d\phi_2
 \end{aligned} \tag{32}$$

where $\chi(\phi_1, \phi_2) = (\sin^2(\pi/M)/\sin^2(\phi_1)) + (\sin^2(\pi/M)/\sin^2(\phi_2))$.

Similar to Part-A, the rest of the three terms in Part-B of (28) can be written as follows:

$$\begin{aligned}
 I'_1 &= I_2(\bar{\gamma}_{R_lD}, \bar{\gamma}_{SR_l}) \\
 I'_2 &= I_1(\bar{\gamma}_{R_lD}, \bar{\gamma}_{SR_l}) \\
 I'_3 &= I_3(\bar{\gamma}_{R_lD}, \bar{\gamma}_{SR_l}, \phi_2, \phi_1).
 \end{aligned} \tag{33}$$

From (27) and (30)–(32), it is observed that the expressions are not in closed form and are represented in the form of simple integrals, which can be numerically evaluated. The error events in the SD and SRD links are mutually exclusive. Therefore, we obtain the end-to-end SEP by adding the individual SEPs of the SD and SRD links, which is given by

$$P_{e_1} = P_{eSD} + \sum_{l=1}^N P_{eSR_lD}. \tag{34}$$

From (34), it is difficult to perform diversity order analysis, since the expressions are not in closed form. Therefore, we derive the closed-form asymptotic SEP expression for S1 by considering binary phase-shift keying (BPSK) signaling, and perform diversity order analysis from the asymptotic SEP expression.

Theorem 1: By considering the BPSK signaling over independent and identically distributed (i.i.d.) Rayleigh fading channels, the asymptotic SEP expression for S1 is given by

$$\begin{aligned}
 P_{e_1}^{asy} &= \frac{2^{N-1} \Gamma(N_t N_r + N - 0.5)}{\sqrt{\pi} \bar{\gamma}^{N_t N_r + N}} (N_t N_r + N) \\
 &\quad + O\left(\frac{1}{\bar{\gamma}^{N_t N_r + N + 1}}\right).
 \end{aligned} \tag{35}$$

Proof: The upper bound on the conditional error probability of BPSK signaling is given by

$$P_e(\gamma) \leq \exp(-\gamma) / \sqrt{4\pi\gamma}. \tag{36}$$

Assuming $\bar{\gamma} = \bar{\gamma}_{SD} = \bar{\gamma}_{SR_j} = \bar{\gamma}_{R_jD}$ and $A = A_j$, where $j = 1, 2, \dots, N$, we substitute (36) in (25) and (28). After approximating the terms $1 - \exp(-At_1) \approx At_1$, $1 - \exp(t_1/\bar{\gamma}) \approx t_1/\bar{\gamma}$, and $1 + (1/\bar{\gamma}) \approx 1$ under the high-SNR condition and neglecting a few insignificant terms, the closed-form asymptotic expression for the i.i.d. case is given by (35).

$$\begin{aligned}
 P_{eSR_lD} &= N_t N_r \left\{ \underbrace{\int_0^\infty \int_{t_3}^\infty P_{eSR_lD}(t_3, t_2) f_{\gamma_{SR_l}}(t_3) f_{\gamma_{R_lD}}(t_2) \prod_{\substack{j=1 \\ j \neq l}}^N F_{V_j}(t_3) \int_0^{t_3} f_{\gamma_{SD}}(t_1) (F_{\gamma_{SD}}(t_1))^{(N_t N_r) - 1} dt_1 dt_2 dt_3}_{\text{Part-A } I_1(\bar{\gamma}_{SR_l}, \bar{\gamma}_{R_lD}) + I_2(\bar{\gamma}_{SR_l}, \bar{\gamma}_{R_lD}) - I_3(\bar{\gamma}_{SR_l}, \bar{\gamma}_{R_lD}, \phi_1, \phi_2)} \right. \\
 &\quad \left. + \underbrace{\int_0^\infty \int_{t_2}^\infty P_{eSR_lD}(t_3, t_2) f_{\gamma_{SR_l}}(t_3) f_{\gamma_{R_lD}}(t_2) \prod_{\substack{j=1 \\ j \neq l}}^N F_{V_j}(t_2) \int_0^{t_2} f_{\gamma_{SD}}(t_1) (F_{\gamma_{SD}}(t_1))^{(N_t N_r) - 1} dt_1 dt_3 dt_2}_{\text{Part-B } I'_1 + I'_2 - I'_3} \right\} \tag{28}
 \end{aligned}$$

Corollary 1: From (35), it is inferred that the diversity order of S1 is $N_t N_r + N$.

C. S2

The average SEP of the SD link is obtained by averaging (24) over the exponential distribution of the SD link under the condition $\gamma_{S_k D_c} > \gamma_t$, and the average is given by

$$P'_{eSD} = N_t N_r \int_{\gamma_t}^{\infty} P_e(t_1) f_{\gamma_{SD}}(t_1) (F_{\gamma_{SD}}(t_1))^{(N_t N_r)-1} dt_1. \quad (37)$$

After substituting (24) and (10) in (37) and solving the integrals, the average SEP of the SD link is given by

$$P'_{eSD} = \frac{N_t N_r}{\pi \bar{\gamma}_{SD}} \sum_{m=0}^{N_t N_r - 1} \binom{N_t N_r - 1}{m} (-1)^m \times \int_0^{\phi_0} \frac{\exp(-\gamma_t \{\chi(\phi) + (m+1)/\bar{\gamma}_{SD}\})}{\{\chi(\phi) + (m+1)/\bar{\gamma}_{SD}\}} d\phi. \quad (38)$$

The average SEP of the SRD link is obtained by averaging (20) over the exponential distribution of the SR and RD links under the condition $\gamma_{S_k D_c} < \gamma_t$. Since we employ SEC combining at D for S2, we assume that the l th relay is selected, where $l \neq N$, under the condition $\min(\gamma_{S_k R_j}, \gamma_{R_j D_c}) < \gamma_t$, where $j = 1, \dots, l-1$, and $\min(\gamma_{S_k R_l}, \gamma_{R_l D_c}) > \gamma_t$. Considering the conditions mentioned, the average SEP of the l th SRD link is given by

$$P'_{eSR_l D} = N_t N_r \prod_{j=1}^{l-1} F_{V_j}(\gamma_t) \int_0^{\gamma_t} f_{\gamma_{SD}}(t_1) (F_{\gamma_{SD}}(t_1))^{(N_t N_r)-1} dt_1 \times \underbrace{\int_{\gamma_t}^{\infty} \int_{\gamma_t}^{\infty} P_{eSR_l D}(t_3, t_2) f_{\gamma_{SR_l}}(t_3) f_{\gamma_{R_l D}}(t_2) dt_2 dt_3}_{J_1 + J_2 - J_3}. \quad (39)$$

By substituting (20), we split (39) into three terms. The first term J_1 is given by

$$J_1 = \int_{\gamma_t}^{\infty} \int_{\gamma_t}^{\infty} P_e(t_3) f_{\gamma_{SR_l}}(t_3) f_{\gamma_{R_l D}}(t_2) dt_2 dt_3. \quad (40)$$

Substituting (24) and (10) in (40) and solving the integrals, we get

$$J_1 = \frac{1}{\pi} \frac{1}{\bar{\gamma}_{SR_l}} \exp\left(\frac{-\gamma_t}{\bar{\gamma}_{SR_l}}\right) \int_0^{\phi_0} \exp(-\gamma_t \chi(\phi, \bar{\gamma}_{SR_l})) \times \{\chi(\phi, \bar{\gamma}_{SR_l})\}^{-1} d\phi. \quad (41)$$

The second and third terms are obtained by substituting $P_e(t_2)$ and $P_e(t_2) P_e(t_3)$, respectively, for $P_e(t_3)$ in (40). After solving the integrals, J_2 and J_3 are, respectively, given by

$$J_2 = \frac{1}{\pi} \frac{1}{\bar{\gamma}_{R_l D}} \exp\left(\frac{-\gamma_t}{\bar{\gamma}_{R_l D}}\right) \times \int_0^{\phi_0} \exp(-\gamma_t \chi(\phi, \bar{\gamma}_{R_l D})) \{\chi(\phi, \bar{\gamma}_{R_l D})\}^{-1} d\phi. \quad (42)$$

$$J_3 = \frac{(J_1 J_2)}{(\exp(-A_l \gamma_t))}.$$

After solving the outer integral in (39) using binomial expansion, the final expression for $P'_{eSR_l D}$ is given by

$$P'_{eSR_l D} = N_t N_r \prod_{j=1}^{l-1} F_{V_j}(\gamma_t) \frac{1}{\bar{\gamma}_{SD}} \sum_{m=0}^{N_t N_r - 1} \binom{N_t N_r - 1}{m} (-1)^m \times \left\{ \frac{1 - \exp\left(-\gamma_t \left\{ \frac{m+1}{\bar{\gamma}_{SD}} \right\}\right)}{\frac{m+1}{\bar{\gamma}_{SD}}} \right\} (J_1 + J_2 - J_3). \quad (43)$$

We assume that the N th relay is selected under the condition $\min(\gamma_{S_k R_j}, \gamma_{R_j D_c}) < \gamma_t$, where $j = 1, 2, \dots, N-1$. Considering the aforementioned condition, the average SEP of the N th SRD link is given by

$$P'_{eSR_N D} = N_t N_r \prod_{j=1}^{N-1} F_{V_j}(\gamma_t) \int_0^{\gamma_t} f_{\gamma_{SD}}(t_1) (F_{\gamma_{SD}}(t_1))^{(N_t N_r)-1} dt_1 \times \underbrace{\int_0^{\infty} \int_0^{\infty} P_{eSR_N D}(t_3, t_2) f_{\gamma_{SR_N}}(t_3) f_{\gamma_{R_N D}}(t_2) dt_2 dt_3}_{J_1 + J_2 - J_3}. \quad (44)$$

By substituting (20), we split (44) into three terms. Similar to J_1 , J_2 , and J_3 , we solve J'_1 , J'_2 , and J'_3 for which the final expressions are given by

$$J'_1 = \frac{1}{\pi} \frac{1}{\bar{\gamma}_{SR_N}} \int_0^{\phi_0} \{\chi(\phi, \bar{\gamma}_{SR_N})\}^{-1} d\phi$$

$$J'_2 = \frac{1}{\pi} \frac{1}{\bar{\gamma}_{R_N D}} \int_0^{\phi_0} \{\chi(\phi, \bar{\gamma}_{R_N D})\}^{-1} d\phi$$

$$J'_3 = J'_1 \times J'_2. \quad (45)$$

After solving the outer integral in (44) using binomial expansion, the final expression for $P'_{eSR_N D}$ is given by

$$P'_{eSR_N D} = N_t N_r \prod_{j=1}^{N-1} F_{V_j}(\gamma_t) \frac{1}{\bar{\gamma}_{SD}} \sum_{m=0}^{N_t N_r - 1} \binom{N_t N_r - 1}{m} (-1)^m \times \left\{ \frac{1 - \exp\left(-\gamma_t \left\{ \frac{m+1}{\bar{\gamma}_{SD}} \right\}\right)}{\frac{m+1}{\bar{\gamma}_{SD}}} \right\} (J'_1 + J'_2 - J'_3). \quad (46)$$

From (38), (43), and (46), the end-to-end SEP expression for S2 is given by

$$P_{e_2} = P'_{eSD} + \sum_{l=1}^{N-1} P'_{eSR_lD} + P'_{eSR_ND}. \quad (47)$$

It is important to note that the individual terms in (47) are not in closed form. Therefore, to perform diversity order analysis, a closed-form asymptotic SEP expression is derived.

Theorem 2: By considering BPSK signaling for S2 over i.i.d. Rayleigh fading channels, the asymptotic SEP expression is given by

$$P_{e_2}^{\text{asy}} \approx \frac{2^{N-1} \gamma_t^{N_t N_r + (N-1)}}{\bar{\gamma}^{N_t N_r + N}} + O\left(\frac{1}{\bar{\gamma}^{N_t N_r + N + 1}}\right). \quad (48)$$

Proof: First, we substitute (36) in (37). After approximating $1 - \exp(-t_l/\bar{\gamma}_{SD}) \approx t_l/\bar{\gamma}_{SD}$ and $1 + (1/\bar{\gamma}_{SD}) \approx 1$ under the high-SNR condition, the closed-form asymptotic SEP expression for the SD link, considering BPSK signaling, is given by

$$P_{eSD}^{\text{asy}} = \frac{N_t N_r \Gamma(N_t N_r - 0.5, \gamma_t)}{2\sqrt{\pi} (\bar{\gamma}_{SD})^{N_t N_r}}. \quad (49)$$

Assuming that $\bar{\gamma}_{SR} = \bar{\gamma}_{SR_j}$ and $\bar{\gamma}_{RD} = \bar{\gamma}_{RD_j}$, $j = 1, 2, \dots, N$, we substitute (36) in (20), and the resultant expression is substituted in (39). After approximating (39) by using $1 + (1/\bar{\gamma}_{SR}) \approx 1$, $1 + (1/\bar{\gamma}_{RD}) \approx 1$, $1 - \exp(-t_l/\bar{\gamma}_{SD}) \approx t_l/\bar{\gamma}_{SD}$, and $1 - \exp(-A\gamma_t) \approx A\gamma_t$ under the high-SNR condition, the asymptotic SEP expression for the l th SRD link considering BPSK signaling is given by

$$P'_{eSR_lD}^{\text{asy}} = N_t N_r (A\gamma_t)^{l-1} \gamma \left(N_t N_r, \frac{\gamma_t}{\bar{\gamma}_{SD}} \right) \times (J_1^{\text{asy}} + J_2^{\text{asy}} - J_3^{\text{asy}}) \quad (50)$$

where $J_1^{\text{asy}} = \exp(-\gamma_t/\bar{\gamma}_{RD}) \Gamma(0.5, \gamma_t)/2\sqrt{\pi} \bar{\gamma}_{SR}$, $J_2^{\text{asy}} = \exp(-\gamma_t/\bar{\gamma}_{SR}) \Gamma(0.5, \gamma_t)/2\sqrt{\pi} \bar{\gamma}_{RD}$, and $J_3^{\text{asy}} = (\Gamma(0.5, \gamma_t))^2/4\pi \bar{\gamma}_{SR} \bar{\gamma}_{RD}$. After high-SNR approximation, the asymptotic SEP expression for the N th SRD link is given by

$$P'_{eSR_ND}^{\text{asy}} = N_t N_r (A\gamma_t)^{N-1} \gamma \left(N_t N_r, \frac{\gamma_t}{\bar{\gamma}_{SD}} \right) \times \left\{ \frac{1}{2} \left(\frac{1}{\bar{\gamma}_{SR}} + \frac{1}{\bar{\gamma}_{RD}} + \frac{1}{2\bar{\gamma}_{RD} \bar{\gamma}_{SR}} \right) \right\}. \quad (51)$$

We add the individual asymptotic SEPs of the SD, l th SRD, and N th SRD links to get the end-to-end asymptotic SEP of S2 for BPSK signaling in closed form. After removing the insignificant terms and approximating $\gamma(N_t N_r, \gamma_t/\bar{\gamma}_{SD}) \approx (\gamma_t/\bar{\gamma}_{SD})^{N_t N_r}/N_t N_r$ under the high-SNR condition [20, eq. (30)], the simplified asymptotic SEP expression for the i.i.d. case (i.e., $\bar{\gamma} = \bar{\gamma}_{SD} = \bar{\gamma}_{SR} = \bar{\gamma}_{RD}$) in closed form is given by (48).

Corollary 2: From (48), it is inferred that the diversity order of S2 is equal to $N_t N_r + N$. Moreover, it is important to note that the asymptotic SEP given by (48) is valid except for the case when $\gamma_t \ll \bar{\gamma}$.

For the case when $\gamma_t \ll \bar{\gamma}$, all the links will be acceptable, and S2 eventually chooses the direct SD link. Hence, the

asymptotic expression for the mentioned case is given by (49), and the diversity order of S2 is equal to $N_t N_r$.

D. S3

The average SEP of the SD link is obtained by considering the following conditions: 1) $\gamma_{S_k D_c} > \gamma_t$; 2) $\gamma_{S_{k'} D_{c'}} < \gamma_t$, where $\{k', c'\} = [\{1, 1\}, \dots, \{k, c-1\}]$; 3) $\min(\gamma_{S_k R_j}, \gamma_{R_j D_c}) < \gamma_t$, where $j = 1, \dots, l-1$, and $l \neq N$; 4) $\min(\gamma_{S_k R_l}, \gamma_{R_l D_c}) > \gamma_t$; and 5) $\gamma_{S_k D_c} > \min(\gamma_{S_k R_l}, \gamma_{R_l D_c})$. The average SEP of the SD link incorporating the aforementioned conditions is given by

$$P_{e_3SD} = \sum_{p=1}^{N_t N_r} (F_{\gamma_{SD}}(\gamma_t))^{p-1} \sum_{l=1}^{N-1} \prod_{j=1}^{l-1} F_{V_j}(\gamma_t) \times \int_{\gamma_t}^{\infty} \int_{t_6}^{\infty} P_e(t_1) f_{\gamma_{SD}}(t_1) f_{V_l}(t_6) dt_6 dt_1. \quad (52)$$

We substitute (24), (10), and (15) in (52) and after solving the integrals, the final expression is given by

$$P_{e_3SD} = \sum_{p=1}^{N_t N_r} (F_{\gamma_{SD}}(\gamma_t))^{p-1} \sum_{l=1}^{N-1} \prod_{j=1}^{l-1} F_{V_j}(\gamma_t) \times \left\{ \frac{A_l}{\pi \bar{\gamma}_{SD}} \int_0^{\phi_0} \{\chi(\phi, \bar{\gamma}_{SD})\}^{-1} \exp\{-\gamma_t(\chi(\phi, \bar{\gamma}_{SD}) + A_l)\} \times \{\chi(\phi, \bar{\gamma}_{SD}) + A_l\}^{-1} d\phi \right\}. \quad (53)$$

Assuming that $l = N$ and $\{k, c\} \neq \{N_t, N_r\}$, we derive the average SEP of the SD link by considering the following conditions: 1) $\gamma_{S_k D_c} > \gamma_t$; 2) $\gamma_{S_{k'} D_{c'}} < \gamma_t$, where $\{k', c'\} = [\{1, 1\}, \dots, \{k, c-1\}]$; 3) $\min(\gamma_{S_k R_j}, \gamma_{R_j D_c}) < \gamma_t$, where $j = 1, 2, \dots, N-1$; and 4) $\gamma_{S_k D_c} > \min(\gamma_{S_k R_N}, \gamma_{R_N D_c})$. The average SEP of the SD link is given by

$$P'_{e_3SD} = \sum_{p=1}^{N_t N_r - 1} (F_{\gamma_{SD}}(\gamma_t))^{p-1} \prod_{j=1}^{N-1} F_{V_j}(\gamma_t) \times \int_{\gamma_t}^{\infty} \int_0^{t_1} P_e(t_1) f_{\gamma_{SD}}(t_1) f_{V_N}(t_7) dt_7 dt_1. \quad (54)$$

After substituting (24), (10), and (15) in (54) and solving the integrals, the average SEP expression is given by

$$P'_{e_3SD} = \sum_{p=1}^{N_t N_r - 1} (F_{\gamma_{SD}}(\gamma_t))^{p-1} \prod_{j=1}^{N-1} F_{V_j}(\gamma_t) \times \frac{1}{\pi \bar{\gamma}_{SD}} \int_0^{\phi_0} \exp\{-\gamma_t \chi(\phi, \bar{\gamma}_{SD})\} \{\chi(\phi, \bar{\gamma}_{SD})\}^{-1} - \exp\{-\gamma_t(\chi(\phi, \bar{\gamma}_{SD}) + A_N)\} \{\chi(\phi, \bar{\gamma}_{SD}) + A_N\}^{-1} d\phi. \quad (55)$$

Assuming that $l = N$ and $\{k, c\} = [\{N_t, N_r\}]$, the average SEP of the SD link can be expressed as

$$P''_{e_3SD} = (F_{\gamma_{SD}}(\gamma_t))^{N_t N_r - 1} \prod_{j=1}^{N-1} F_{V_j}(\gamma_t) \times \int_0^\infty \int_0^{t_1} P_e(t_1) f_{\gamma_{SD}}(t_1) f_{V_N}(t_7) dt_7 dt_1. \quad (56)$$

After solving the integrals in (56), the average SEP expression for the SD link is given by

$$P''_{e_3SD} = \frac{(F_{\gamma_{SD}}(\gamma_t))^{N_t N_r - 1} \prod_{j=1}^{N-1} F_{V_j}(\gamma_t)}{\pi \bar{\gamma}_{SD}} \times \int_0^{\phi_0} (\{\chi(\phi, \bar{\gamma}_{SD})\}^{-1} - \{\chi(\phi, \bar{\gamma}_{SD}) + A_N\}^{-1}) d\phi. \quad (57)$$

From (53), (55), and (57), the average SEP of the SD link for S3 is given by

$$P''_{eSD} = P_{e_3SD} + P'_{e_3SD} + P''_{e_3SD}. \quad (58)$$

The average SEP of the SRD link is obtained by averaging (20) over the exponential distribution of the SR and RD links by considering the following conditions: 1) $\gamma_{S_k D_c} > \gamma_t$, where $\{k, c\} \neq [\{N_t, N_r\}]$; 2) $\gamma_{S_{k'} D_{c'}} < \gamma_t$, where $\{k', c'\} = [\{1, 1\}, \dots, \{k, c-1\}]$; 3) $\min(\gamma_{S_k R_j}, \gamma_{R_j D_c}) < \gamma_t$, where $j = 1, \dots, l-1$; 4) $\min(\gamma_{S_k R_l}, \gamma_{R_l D_c}) > \gamma_t$, where $l = 1, 2, \dots, N$; and 5) $\min(\gamma_{S_k R_l}, \gamma_{R_l D_c}) > \gamma_{S_k D_c}$. Hence, the

average SEP expression for the SRD link is given by (59), shown at the bottom of the page, and we split the expression into six terms. The first term B_1 is given by

$$B_1(\bar{\gamma}_{SR_l}, \bar{\gamma}_{R_l D}) = \int_{\gamma_t}^\infty \int_{t_1}^\infty \int_{t_3}^\infty P_e(t_3) f_{\gamma_{SR_l}}(t_3) \times f_{\gamma_{R_l D}}(t_2) f_{\gamma_{SD}}(t_1) dt_2 dt_3 dt_1. \quad (60)$$

Substituting (24) and (10) in (60) and solving the integrals results in

$$B_1(\bar{\gamma}_{SR_l}, \bar{\gamma}_{R_l D}) = \int_0^{\phi_0} \frac{\exp\{-\gamma_t (\chi(\phi, \bar{\gamma}_{SD}) + A_l)\}}{\pi \bar{\gamma}_{SR_l} \bar{\gamma}_{R_l D} (\chi(\phi) + A_l) (\chi(\phi, \bar{\gamma}_{SD}) + A_l)} d\phi. \quad (61)$$

The second term B_2 and the third term B_3 can be obtained by substituting $P_e(t_2)$ and $P_e(t_2) P_e(t_3)$, respectively, for $P_e(t_3)$ in (60). After solving the integrals, B_2 and B_3 are given, respectively, by (62) and (63), shown at the bottom of the page. From (63), $\chi(\phi_1, \phi_2, \bar{\gamma}_{ii}) = (\sin^2(\pi/M)/\sin^2(\phi_1)) + (\sin^2(\pi/M)/\sin^2(\phi_2)) + (1/\bar{\gamma}_{ii})$. The final three terms B'_1, B'_2 , and B'_3 can be written from $B_1(\cdot, \cdot), B_2(\cdot, \cdot)$, and $B_3(\cdot, \cdot, \cdot, \cdot)$, as given by

$$\begin{aligned} B'_1 &= B_2(\bar{\gamma}_{R_l D}, \bar{\gamma}_{SR_l}) \\ B'_2 &= B_1(\bar{\gamma}_{R_l D}, \bar{\gamma}_{SR_l}) \\ B'_3 &= B_3(\bar{\gamma}_{R_l D}, \bar{\gamma}_{SR_l}, \phi_2, \phi_1). \end{aligned} \quad (64)$$

$$P_{e_3SRD} = \sum_{p=1}^{N_t N_r - 1} (F_{\gamma_{SD}}(\gamma_t))^{p-1} \sum_{l=1}^N \prod_{j=1}^{l-1} F_{V_j}(\gamma_t) \left\{ \underbrace{\int_{\gamma_t}^\infty \int_{t_1}^\infty \int_{t_3}^\infty P_{eSR_l D}(t_3, t_2) f_{\gamma_{SR_l}}(t_3) f_{\gamma_{R_l D}}(t_2) f_{\gamma_{SD}}(t_1) dt_2 dt_3 dt_1}_{B_1(\bar{\gamma}_{SR_l}, \bar{\gamma}_{R_l D}) + B_2(\bar{\gamma}_{SR_l}, \bar{\gamma}_{R_l D}) - B_3(\bar{\gamma}_{SR_l}, \bar{\gamma}_{R_l D}, \phi_1, \phi_2)} + \underbrace{\int_{\gamma_t}^\infty \int_{t_1}^\infty \int_{t_2}^\infty P_{eSR_l D}(t_3, t_2) f_{\gamma_{SR_l}}(t_3) f_{\gamma_{R_l D}}(t_2) f_{\gamma_{SD}}(t_1) dt_3 dt_2 dt_1}_{B'_1 + B'_2 - B'_3} \right\} \quad (59)$$

$$B_2(\bar{\gamma}_{SR_l}, \bar{\gamma}_{R_l D}) = \int_0^{\phi_0} \frac{\exp\{-\gamma_t (\chi(\phi, \bar{\gamma}_{SD}) + A_l)\}}{\pi \bar{\gamma}_{SR_l} \bar{\gamma}_{R_l D} \bar{\gamma}_{SD} (\chi(\phi) + A_l) (\chi(\phi, \bar{\gamma}_{R_l D})) (\chi(\phi, \bar{\gamma}_{SD}) + A_l)} d\phi \quad (62)$$

$$B_3(\bar{\gamma}_{SR_l}, \bar{\gamma}_{R_l D}, \phi_1, \phi_2) = \int_0^{\phi_0} \int_0^{\phi_0} \frac{\exp\{-\gamma_t (\chi(\phi_1, \phi_2, \bar{\gamma}_{SD}) + A_l)\}}{\pi^2 \bar{\gamma}_{SR_l} \bar{\gamma}_{R_l D} \bar{\gamma}_{SD} (\chi(\phi_1, \phi_2) + A_l) (\chi(\phi_2, \bar{\gamma}_{R_l D})) (\chi(\phi_1, \phi_2, \bar{\gamma}_{SD}) + A_l)} d\phi_1 d\phi_2 \quad (63)$$

From (59), it is observed that we have not considered the case $\{k, c\} = [\{N_t, N_r\}]$. Assuming that $\{k, c\} = [\{N_t, N_r\}]$, the average SEP of the SRD link is obtained by considering the following conditions: 1) $\gamma_{S_{k'}D_{c'}} < \gamma_t$, where $\{k', c'\} = [\{1, 1\}, \dots, \{N_t, N_r - 1\}]$; 2) $\min(\gamma_{S_{N_t}R_j}, \gamma_{R_jD_{N_r}}) < \gamma_t$, where $j = 1, \dots, l - 1$; 3) $\min(\gamma_{S_{N_t}R_l}, \gamma_{R_lD_{N_r}}) > \gamma_t$, where $l \neq N$; and 4) $\min(\gamma_{S_{N_t}R_l}, \gamma_{R_lD_{N_r}}) > \gamma_{S_{N_t}D_{N_r}}$. The average SEP expression for the SRD link is given by (65), shown at the bottom of the page. We split (65) into six terms. Since the derivation steps are similar to (59), we skip that expression so that the final expressions are given by (66)–(69). Thus

$$C_1(\bar{\gamma}_{SR_l}, \bar{\gamma}_{R_lD}) = \frac{1}{\pi \bar{\gamma}_{SR_l}} \int_0^{\phi_0} \left(\frac{\exp\{-\gamma_t(\chi(\phi) + A_l)\}}{\chi(\phi) + A_l} - \frac{\exp\{-\gamma_t(\chi(\phi, \bar{\gamma}_{SD}) + A_l)\}}{\chi(\phi, \bar{\gamma}_{SD}) + A_l} \right) d\phi \quad (66)$$

$$C_2(\bar{\gamma}_{SR_l}, \bar{\gamma}_{R_lD}) = \frac{1}{\pi \bar{\gamma}_{SR_l} \bar{\gamma}_{R_lD}} \int_0^{\phi_0} \left(\frac{\exp\{-\gamma_t(\chi(\phi) + A_l)\}}{\chi(\phi, \bar{\gamma}_{R_lD})(\chi(\phi) + A_l)} - \frac{\exp\{-\gamma_t(\chi(\phi, \bar{\gamma}_{SD}) + A_l)\}}{\chi(\phi, \bar{\gamma}_{R_lD})(\chi(\phi, \bar{\gamma}_{SD}) + A_l)} \right) d\phi \quad (67)$$

$$C_3(\bar{\gamma}_{SR_l}, \bar{\gamma}_{R_lD}, \phi_1, \phi_2) = \frac{1}{\pi^2 \bar{\gamma}_{SR_l} \bar{\gamma}_{R_lD}} \times \int_0^{\phi_0} \int_0^{\phi_0} \left\{ \frac{\exp\{-\gamma_t(\chi(\phi_1, \phi_2) + A_l)\}}{\chi(\phi_2, \bar{\gamma}_{R_lD})(\chi(\phi_1, \phi_2) + A_l)} - \frac{\exp\{-\gamma_t(\chi(\phi_1, \phi_2, \bar{\gamma}_{SD}) + A_l)\}}{\chi(\phi_2, \bar{\gamma}_{R_lD})(\chi(\phi_1, \phi_2, \bar{\gamma}_{SD}) + A_l)} \right\} d\phi_1 d\phi_2 \quad (68)$$

$$C'_1 = C_2(\bar{\gamma}_{R_lD}, \bar{\gamma}_{SR_l}), \quad C'_2 = C_1(\bar{\gamma}_{R_lD}, \bar{\gamma}_{SR_l}) \\ C'_3 = C_3(\bar{\gamma}_{R_lD}, \bar{\gamma}_{SR_l}, \phi_2, \phi_1). \quad (69)$$

It is observed that (65) does not consider the case $l = N$. Therefore, assuming that $l = N$ and $\{k, c\} = [\{N_t, N_r\}]$, the average SEP expression for the SRD link after skipping detailed derivation steps is given by (70), shown at the bottom of the page. The final expressions for all the six terms, skipping the detailed derivation steps, are given by

$$D_1(\bar{\gamma}_{SR_N}, \bar{\gamma}_{R_ND}) = \frac{1}{\pi \bar{\gamma}_{SR_N}} \int_0^{\phi_0} \left\{ (\chi(\phi) + A_N)^{-1} - (\chi(\phi, \bar{\gamma}_{SD}) + A_N)^{-1} \right\} d\phi \quad (71)$$

$$P'_{e_{3SRD}} = (F_{\gamma_{SD}}(\gamma_t))^{N_t N_r - 1} \sum_{l=1}^{N-1} \prod_{j=1}^{l-1} F_{V_j}(\gamma_t) \left\{ \underbrace{\int_0^{t_3} \int_{\gamma_t}^{\infty} \int_{t_3}^{\infty} P_{eSR_lD}(t_3, t_2) f_{\gamma_{SR_l}}(t_3) f_{\gamma_{R_lD}}(t_2) f_{\gamma_{SD}}(t_1) dt_2 dt_3 dt_1}_{C_1(\bar{\gamma}_{SR_l}, \bar{\gamma}_{R_lD}) + C_2(\bar{\gamma}_{SR_l}, \bar{\gamma}_{R_lD}) - C_3(\bar{\gamma}_{SR_l}, \bar{\gamma}_{R_lD}, \phi_1, \phi_2)} \right. \\ \left. + \underbrace{\int_0^{t_2} \int_{\gamma_t}^{\infty} \int_{t_2}^{\infty} P_{eSR_lD}(t_3, t_2) f_{\gamma_{SR_l}}(t_3) f_{\gamma_{R_lD}}(t_2) f_{\gamma_{SD}}(t_1) dt_3 dt_2 dt_1}_{C'_1 + C'_2 - C'_3} \right\} \quad (65)$$

$$P''_{e_{3SRD}} = (F_{\gamma_{SD}}(\gamma_t))^{N_t N_r - 1} \prod_{j=1}^{N-1} F_{V_j}(\gamma_t) \left\{ \underbrace{\int_0^{t_3} \int_0^{\infty} \int_{t_3}^{\infty} P_{eSR_ND}(t_3, t_2) f_{\gamma_{SR_N}}(t_3) f_{\gamma_{R_ND}}(t_2) f_{\gamma_{SD}}(t_1) dt_2 dt_3 dt_1}_{D_1(\bar{\gamma}_{SR_N}, \bar{\gamma}_{R_ND}) + D_2(\bar{\gamma}_{SR_N}, \bar{\gamma}_{R_ND}) - D_3(\bar{\gamma}_{SR_N}, \bar{\gamma}_{R_ND}, \phi_1, \phi_2)} \right. \\ \left. + \underbrace{\int_0^{t_2} \int_0^{\infty} \int_{t_2}^{\infty} P_{eSR_ND}(t_3, t_2) f_{\gamma_{SR_N}}(t_3) f_{\gamma_{R_ND}}(t_2) f_{\gamma_{SD}}(t_1) dt_3 dt_2 dt_1}_{D'_1 + D'_2 - D'_3} \right\} \quad (70)$$

$$D_2(\bar{\gamma}_{SR_N}, \bar{\gamma}_{R_N D}) = \frac{1}{\pi \bar{\gamma}_{SR_N} \bar{\gamma}_{R_N D}} \int_0^{\phi_0} (\chi(\phi, \bar{\gamma}_{R_N D}))^{-1} \times \left\{ (\chi(\phi) + A_N)^{-1} - (\chi(\phi, \bar{\gamma}_{SD}) + A_N)^{-1} \right\} d\phi \quad (72)$$

$$D_3(\bar{\gamma}_{SR_N}, \bar{\gamma}_{R_N D}, \phi_1, \phi_2) = \frac{1}{\pi^2 \bar{\gamma}_{SR_N} \bar{\gamma}_{R_N D}} \int_0^{\phi_0} \int_0^{\phi_0} (\chi(\phi_2, \bar{\gamma}_{R_N D}))^{-1} \times \left\{ (\chi(\phi_1, \phi_2) + A_N)^{-1} - (\chi(\phi_1, \phi_2, \bar{\gamma}_{SD}) + A_N)^{-1} \right\} d\phi_1 d\phi_2 \quad (73)$$

$$D'_1 = D_2(\bar{\gamma}_{R_N D}, \bar{\gamma}_{SR_N}), \quad D'_2 = D_1(\bar{\gamma}_{R_N D}, \bar{\gamma}_{SR_N}) \\ D'_3 = D_3(\bar{\gamma}_{R_N D}, \bar{\gamma}_{SR_N}, \phi_2, \phi_1). \quad (74)$$

Finally, from (59), (65), and (70), the average SEP of the SRD link for S3 is given by

$$P''_{eSRD} = P_{e3SRD} + P'_{e3SRD} + P''_{e3SRD}. \quad (75)$$

The individual terms in P''_{eSD} and P''_{eSRD} are not given in closed form and are represented in the form of simple integrals, which can be numerically evaluated. From (58) and (75), the average end-to-end SEP of S3 is given by

$$P_{e3} = P''_{eSD} + P''_{eSRD}. \quad (76)$$

Neglecting the P_{e3SD} and P'_{e3SD} terms under the high-SNR condition, the asymptotic SEP of the SD link depends on the P''_{e3SD} term. Using high-SNR approximations as mentioned in S1 and S2, the simplified asymptotic SEP of the SD link for the i.i.d. case is given by

$$P''_{e3SD}{}^{asy} = \frac{2^{N-2} \gamma_t^{(N_t N_r) + N - 2}}{\bar{\gamma}^{N_t N_r + N}}. \quad (77)$$

The asymptotic SEP of the SRD link also mainly depends on the P''_{e3SRD} term, which is given by (70). After high-SNR approximations, the simplified asymptotic SEP of the SRD link is given by

$$P''_{e3SRD}{}^{asy} = \frac{2^{N-2} \gamma_t^{(N_t N_r) + N - 2}}{\bar{\gamma}^{N_t N_r + N}} + O\left(\frac{1}{\bar{\gamma}^{N_t N_r + N + 1}}\right). \quad (78)$$

After summing (77) and (78), the end-to-end asymptotic SEP of S3 in closed form for BPSK signaling is given by

$$P_{e3}{}^{asy} = \frac{2^{N-1} \gamma_t^{(N_t N_r) + N - 2}}{\bar{\gamma}^{N_t N_r + N}} + O\left(\frac{1}{\bar{\gamma}^{N_t N_r + N + 1}}\right). \quad (79)$$

Neglecting the least significant higher-order term from (79), it is inferred that the diversity order of $N_t N_r + N$ can be achieved using S3. However, similar to S2, the diversity order is obtained except for the case when $\gamma_t \ll \bar{\gamma}$. For the mentioned case, $\gamma_{S_1 D_1} > \gamma_t$ and $\min(\gamma_{S_1 R_1}, \gamma_{R_1 D_1}) > \gamma_t$, and SC will be employed between the SD and SRD links. Therefore, the diversity order for the case when $\gamma_t \ll \bar{\gamma}$ will be reduced to 2.

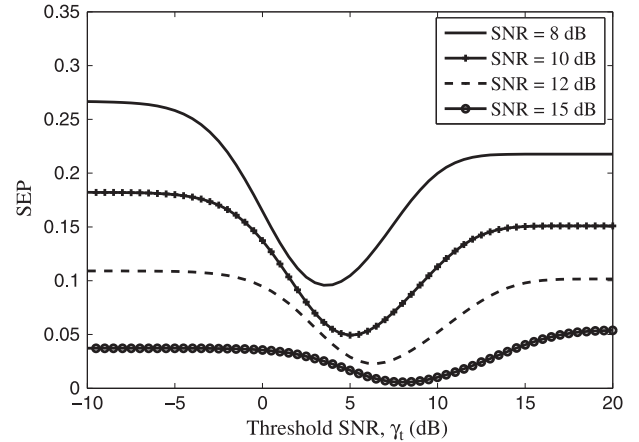


Fig. 2. Threshold SNR optimization for different average SNR values by considering S2, assuming that $M = 4$ and $N = N_t = N_r = 3$.

V. IMPACT OF OUTDATED/DELAYED CSI

In the case of the antenna selection strategy, the CSI of SD links is estimated at D, and from the instantaneous SNR values of SD links, the transmit–receive antenna pair is selected. The selected transmit antenna index is sent back to the transmitter via a noiseless feedback link. Although perfect CSI of SD links is estimated at D, due to nonzero feedback delay and delay due to relay selection in the guard period, the transmit antenna at S and path selection at D could be chosen based on outdated CSI of SD links. Hence, the relationship between outdated/delayed CSI $\hat{h}_{S_k D_c}$ and actual $h_{S_k D_c}$ is given by [21]

$$h_{S_k D_c} = \rho \hat{h}_{S_k D_c} + \sqrt{1 - \rho^2} w \quad (80)$$

where ρ is the correlation coefficient between the outdated and actual channel, and w is modeled as a complex Gaussian RV with zero mean and unit variance. Here, $\rho = 1$ means path, and antenna selection is based on actual CSI with no delay, and $\rho = 0$ means no CSI is available; therefore diversity gain cannot be obtained. The impact of the delayed/outdated CSI is studied using Monte Carlo simulation.

VI. NUMERICAL RESULTS AND DISCUSSIONS

First, all of the SEP performance curves except those in Fig. 8 are plotted by assuming that $\bar{\gamma} = \bar{\gamma}_{SD} = \bar{\gamma}_{R_j D} = \bar{\gamma}_{SR_j}$, where $j = 1, 2, \dots, N$. The optimum values of the threshold SNR (i.e., γ_t^{opt}) for different values of the average SNR, which minimize the average SEP values, are numerically obtained as shown in Fig. 2. It is observed that as the value of average SNR increases, the optimum switching threshold SNR value also increases.

The SEP performance curves for four different values of γ_t are shown for S2 and S3 in Figs. 3 and 4, respectively, assuming a quaternary phase-shift keying (QPSK) modulation scheme. From the figures, it is observed that with $\gamma_t = \gamma_t^{\text{opt}}$, systems perform the best. Moreover, as the value of γ_t increases, degradation in the SEP performance also increases. From the plots, it is noticed that the exact SEP values well agree with the simulated SEP values.

In Fig. 5, the asymptotic and exact SEP performance curves are compared for the diversity-optimal and suboptimal strategies by considering the BPSK signaling scheme that assumes

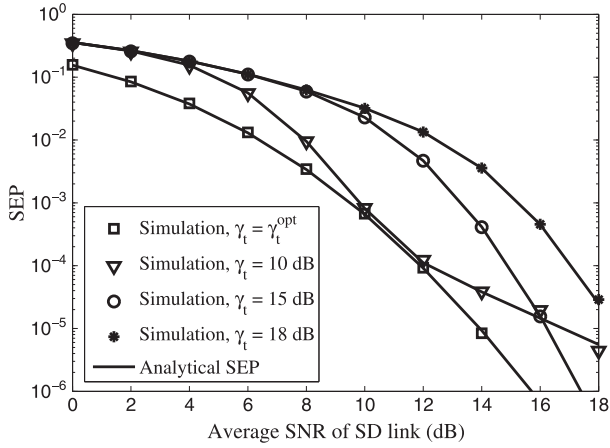


Fig. 3. SEP performance of S2 for four different threshold SNR values, assuming that $M = 4$ and $N_t = N_r = N = 2$.

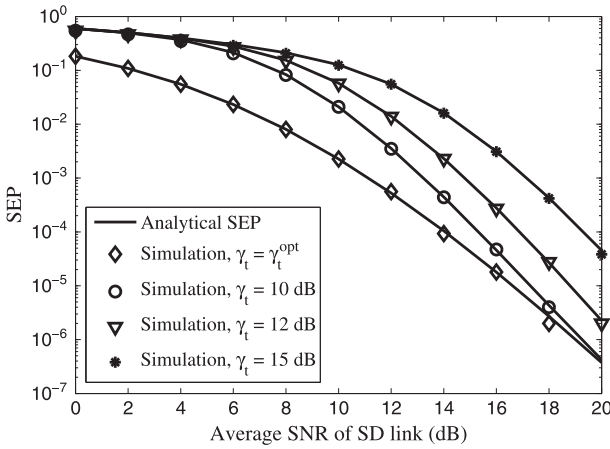


Fig. 4. SEP performance of S3 for four different threshold SNR values, assuming that $M = 4$ and $N_t = N_r = N = 3$.

$\gamma_t = \gamma_t^{\text{opt}}$ and $\gamma_t = 16$ dB for S2 and S3, respectively. From the figure, it is observed that the asymptotic and the exact SEP performance curves closely agree with each other in the high-SNR region. It is also inferred that the diversity order of $N_t N_r + N$ and $N_t N_r + N \min(N_t, N_r)$ is obtained for the suboptimal and diversity-optimal schemes, respectively. From the asymptotic SEP performance of S2 plotted in Fig. 6, it is inferred that with $\gamma_t = 10.5$ dB, S2 offers diversity order of $N_t N_r + N$ in the region of operation of interest. Moreover, the diversity order of S2 converges to $N_t N_r$ in the region where $\gamma_t \ll \bar{\gamma}$ for the $\gamma_t = 5$ dB case.

Given the complicated form of SEP expression, it is evident that the optimization cannot be analytically conducted by deriving a closed-form expression for γ_t^{opt} . Since performing numerical optimization of γ_t for all average SNR values will be complicated at D, we suggest a less complicated method to determine the value of γ_t . Instead of finding the optimum values of γ_t for all average SNR values, we can determine the optimum value of γ_t for one particular high-SNR value similar to [22]. For example, the optimum value of γ_t , which minimizes the average SEP, for $\bar{\gamma} = 35$ dB by considering S2 that assumes $M = 2, N = 2, N_t = 2$, and $N_r = 1$ is equal to 10.5 dB. Hence, by fixing $\gamma_t = 10.5$ dB, the diversity order of $N_t N_r + N$ is obtained in Fig. 6. As γ_t is fixed, degradation in the diversity

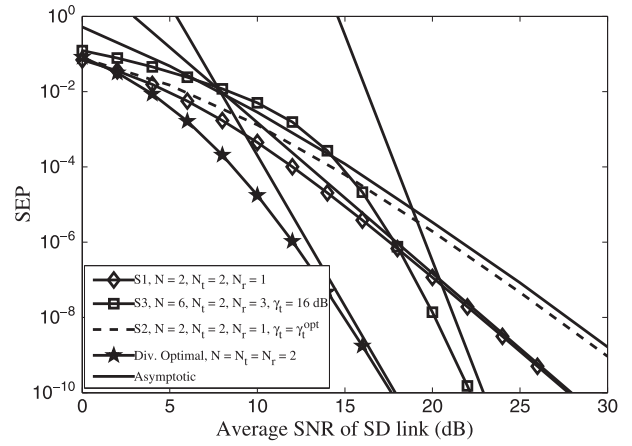


Fig. 5. Comparison of asymptotic and exact SEP values of suboptimal and diversity-optimal schemes, considering $M = 2$.

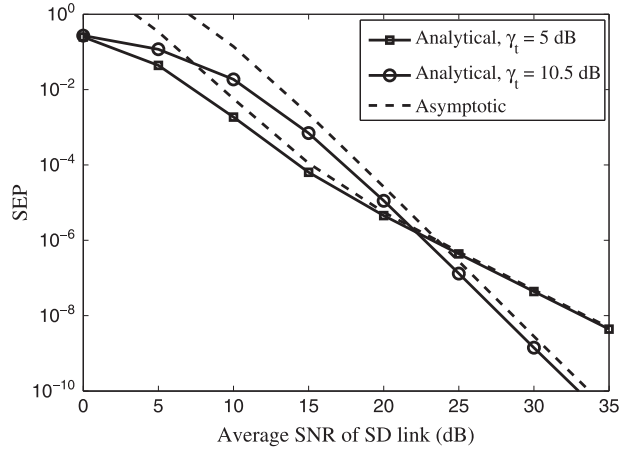


Fig. 6. Comparison of asymptotic and exact SEP values of S2, assuming that $M = 2, N = N_t = 2$, and $N_r = 1$.

order might be observed at the very high-SNR region above 40 dB for the $\gamma_t = 10.5$ dB case. Since in practical systems the receiver does not operate at a very high SNR, the effect in those scenarios can be neglected. Moreover, by fixing $\gamma_t < \gamma_t^{\text{opt}/35}$, where $\gamma_t^{\text{opt}/35}$ denotes the optimum value of γ_t for $\bar{\gamma} = 35$ dB, degradation in the diversity order is obtained in the region of operation of interest as shown in Fig. 6 for the $\gamma_t = 5$ dB case. The reason for degradation in the diversity order is already discussed while deriving the asymptotic SEP expression for S2. Note that the SEP performance of the $\gamma_t = 5$ dB case is better than that of the $\gamma_t = 10.5$ dB case in the low-SNR region less than 20 dB. However, in the high-SNR region above 20 dB, performance improvement is observed for the $\gamma_t = 10.5$ dB case.

Therefore, by fixing $\gamma_t \geq \gamma_t^{\text{opt}/35}$, performance improvement in the high-SNR region along with diversity benefit is obtained compared with that in the $\gamma_t < \gamma_t^{\text{opt}/35}$ case. Furthermore, by fixing $\gamma_t < \gamma_t^{\text{opt}/35}$, performance improvement in the low-SNR region along with degradation in the diversity order is obtained. Because of diversity order degradation, less CSI estimations will be required at D compared with the $\gamma_t \geq \gamma_t^{\text{opt}/35}$ case. Finally, by fixing the threshold SNR value, determining the optimum values for all average SNR values can be avoided, however, at the expense of performance degradation.

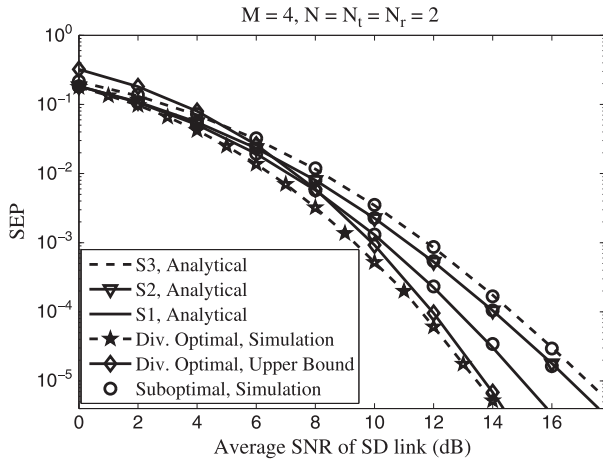


Fig. 7. Comparison of simulated and theoretical SEP values over identical fading channels, assuming that $M = 4$ and $N_t = N_r = N = 2$.

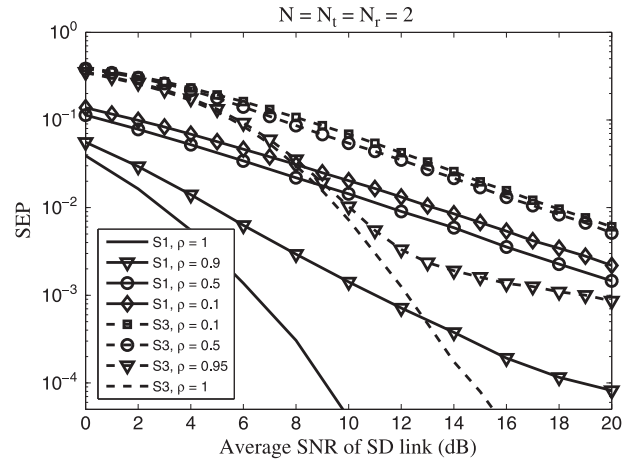


Fig. 9. Average SEP performance of S1 and S3 with outdated/delayed CSI of the SD link, assuming that $N_t = N_r = N = 2$.

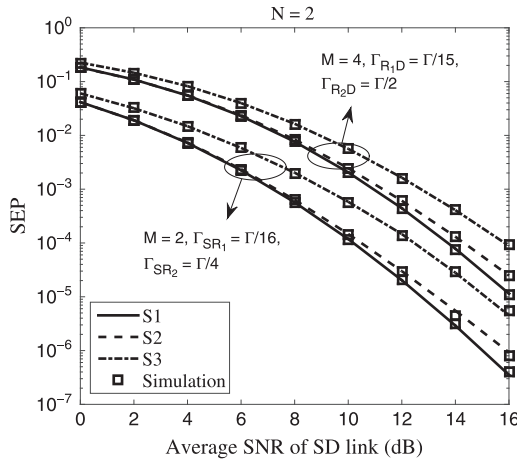


Fig. 8. Comparison of simulated and theoretical SEP values over nonidentical fading channels assuming that $N_t = N_r = N = 2$.

TABLE I
NUMBER OF CSI REQUIRED AT D FOR IDENTICAL FADING SCENARIO, ASSUMING $\gamma_t = \gamma_t^{opt}$, $M = 4$, AND $N = N_t = N_r = 3$

SNR (dB)	No. of CSI required at D			
	Diversity optimal	S1	S2	S3
5	27	15	9.0010	8.9
10	27	15	9.0001	7.5
15	27	15	9	5.7
20	27	15	9	4.6

In Figs. 7 and 8, simulated and theoretical SEP values are compared over identical and nonidentical Rayleigh fading scenarios, respectively, assuming that $\gamma_t = \gamma_t^{opt}$. From both figures, it is observed that for all the suboptimal strategies, the simulated SEP values obtained from Monte Carlo simulations well agree with the theoretical SEP values. Moreover, the upper-bound SEP performance curve of the diversity-optimal strategy closely agrees with the exact performance curve obtained from the Monte Carlo simulations.

In Fig. 7, it is observed that S1 performs better than S2 and S3. Note that the antenna and relay selection decision rules used in S1 select the best antenna pair and relay among $N_t N_r + 2N$ links. Since S2 and S3 require less than $N_t N_r + 2N$ links to select the best antenna pair and relay, degradation in the SEP performance is observed compared with S1. In addition, the average number of CSI required at D is compared in Table I

for the identical Rayleigh fading scenario, and the tabulated values are obtained from Monte Carlo simulations. The average number of CSI required at D for S1 is comparatively higher than S2 and S3, as shown in Table I. Therefore, considerable improvement in the SEP performance of S1 is obtained at the cost of increase in the complexity of the system.

It is also inferred from Fig. 7 that the SEP performance of S2 is better than that of S3. It is worth noting that the antenna selection decision rule for S2 is given by (8), and the decision rule for S3 is based on the SEC scheme. Since the antenna selection decision rule employed in S2 selects the best antenna pair among all possible $N_t N_r$ SD links in contrast to the SEC-based antenna selection rule employed in S3, the SEP performance of S2 is better than that of S3 with more CSI requirement at D, as shown in Table I. Finally, the SEP performance of the diversity-optimal strategy is also compared with all the suboptimal strategies in Fig. 7, and considerable performance improvement (i.e., more than 2 dB at 10^{-4}) is observed in the case of the diversity-optimal strategy compared with the suboptimal strategies. However, the diversity-optimal strategy requires the CSI of $N_t N_r + N N_t + N N_r$ links at D to achieve the improved error performance compared with the suboptimal strategies, which require CSI of maximum $N_t N_r + 2N$ links at D, as shown in Table I.

In Fig. 8, the SEP performance curves are plotted and compared over nonidentical Rayleigh fading channels, assuming that $N_t = N_r = N = 2$ and $M = 2$ and 4. Findings from the numerical results that consider the nonidentical average SNR scenario among S-R channels (i.e., $\bar{\gamma}_{SR1} = \bar{\gamma}_1$ and $\bar{\gamma}_{SR2} = \bar{\gamma}_2$, where $\bar{\gamma}_1 = \bar{\gamma}/16$, $\bar{\gamma}_2 = \bar{\gamma}/4$, and $\bar{\gamma} = \bar{\gamma}_{SD} = \bar{\gamma}_{R_j D}$) reveal that the SEP performance of S2 is better than that of S3, similar to the identical fading scenario. In addition, for the case assuming nonidentical channel behavior among R-D channels (i.e., $\bar{\gamma}_{R1D} = \bar{\gamma}_1$ and $\bar{\gamma}_{R2D} = \bar{\gamma}_2$, where $\bar{\gamma}_1 = \bar{\gamma}/15$, $\bar{\gamma}_2 = \bar{\gamma}/2$, and $\bar{\gamma} = \bar{\gamma}_{SD} = \bar{\gamma}_{SR_j}$), the performance trends are similar to those of the previous case. Furthermore, as expected, S1 performs better than S2 and S3 for all the cases. Finally, the Monte Carlo simulation results well agree with the theoretical SEP values.

Fig. 9 shows the impact of the outdated/delayed CSI of the SD link on the average SEP performance of BPSK and QPSK modulation schemes that consider S1 and S3, respectively. From the performance curves, it is inferred that the outdated

$$\begin{aligned}
A_1(\bar{\gamma}_{\text{SR}}, \bar{\gamma}_{\text{RD}}) &\leq \frac{N_t N_r (M-1)}{M \bar{\gamma}_{\text{SR}} \bar{\gamma}_{\text{RD}}} \sum_{m=0}^{N_t N_r} \sum_{k=0}^{N_r-1} \sum_{r=0}^{N_t-1} \binom{N_t N_r}{m} \binom{N_r-1}{k} \binom{N_t-1}{r} \\
&\quad \times (-1)^{m+k+r} \left\{ \sum_{p=0}^{N_t(N-1)} \binom{N_t(N-1)}{p} \frac{(-1)^p}{\left(\sin^2\left(\frac{\pi}{M}\right) + \frac{r+1}{\bar{\gamma}_{\text{SR}}}\right) \left(\sin^2\left(\frac{\pi}{M}\right) + \frac{m}{\bar{\gamma}_{\text{SD}}} + \frac{p+r+1}{\bar{\gamma}_{\text{SR}}} + \frac{k+1}{\bar{\gamma}_{\text{RD}}}\right)} \right. \\
&\quad \left. + \sum_{q=0}^{N_r(N-1)} \binom{N_r(N-1)}{q} \frac{(-1)^q}{\left(\sin^2\left(\frac{\pi}{M}\right) + \frac{r+1}{\bar{\gamma}_{\text{SR}}}\right) \left(\sin^2\left(\frac{\pi}{M}\right) + \frac{m}{\bar{\gamma}_{\text{SD}}} + \frac{r+1}{\bar{\gamma}_{\text{SR}}} + \frac{q+k+1}{\bar{\gamma}_{\text{RD}}}\right)} \right\} \quad (81a)
\end{aligned}$$

$$\begin{aligned}
A_2(\bar{\gamma}_{\text{SR}}, \bar{\gamma}_{\text{RD}}) &\leq \frac{N_t N_r (M-1)}{M \bar{\gamma}_{\text{SR}} \bar{\gamma}_{\text{RD}}} \sum_{m=0}^{N_t N_r} \sum_{k=0}^{N_r-1} \sum_{r=0}^{N_t-1} \binom{N_t N_r}{m} \binom{N_r-1}{k} \binom{N_t-1}{r} \\
&\quad \times \frac{(-1)^{m+k+r} \bar{\gamma}_{\text{SR}}}{r+1} \left\{ \sum_{p=0}^{N_t(N-1)} \binom{N_t(N-1)}{p} \frac{(-1)^p}{\left(\sin^2\left(\frac{\pi}{M}\right) + \frac{m}{\bar{\gamma}_{\text{SD}}} + \frac{p+r+1}{\bar{\gamma}_{\text{SR}}} + \frac{k+1}{\bar{\gamma}_{\text{RD}}}\right)} \right. \\
&\quad \left. + \sum_{q=0}^{N_r(N-1)} \binom{N_r(N-1)}{q} \frac{(-1)^q}{\left(\sin^2\left(\frac{\pi}{M}\right) + \frac{m}{\bar{\gamma}_{\text{SD}}} + \frac{r+1}{\bar{\gamma}_{\text{SR}}} + \frac{q+k+1}{\bar{\gamma}_{\text{RD}}}\right)} \right\} \quad (82a)
\end{aligned}$$

CSI degrades the SEP performance to a greater extent. For example, outdated CSI with $\rho = 0.9$, which S1 requires more than 4-dB SNR to achieve an SEP value of 10^{-3} when compared with the $\rho = 1$ case. Furthermore, the performance degradation is more significant for $\rho \geq 0.5$.

Based on the SC decision rule, the direct or the cooperative path is selected in the case of the diversity-optimal strategy, S1, and S3. If the direct path is chosen, the symbol will be transmitted in one time slot. However, if the cooperative path is selected, spectral efficiency is reduced to half because two time slots are required. Moreover, the probability of selection of either the direct or the cooperative path is equal for the diversity-optimal strategy, S1, and S3. In the case of S2, the direct path is compared with the threshold SNR, and if the condition is satisfied, then the cooperative path is neglected. Note that the direct path is also compared with the threshold SNR in S3. However, if the condition is satisfied, the direct path will be compared with the best cooperative path, which satisfies the threshold SNR condition unlike S2. In addition to that, for the case when $\gamma_t \ll \bar{\gamma}$, all the links will be acceptable, and S2 eventually chooses the direct SD link most of the time. Therefore, S2 is the most spectrally efficient strategy compared with other strategies.

VII. CONCLUSION

In this paper, the average SEP expressions are derived for a diversity-optimal and three different suboptimal transmit–receive antenna and relay selection strategies that consider a DF multirelay system over Rayleigh fading channels, assuming MPSK signaling. Moreover, the diversity order analysis is performed by deriving the closed-form asymptotic SEP expressions. From the derived asymptotic expressions, it is observed that the diversity-optimal strategy achieves full diversity order of $N_t N_r + N \min(N_t, N_r)$. However, all three suboptimal strategies achieve diversity order of $N_t N_r + N$, except for the case when $\gamma_t \ll \bar{\gamma}$ in S2 and S3. By considering S2 and S3, the diversity order for the case when $\gamma_t \ll \bar{\gamma}$ is equal to $N_t N_r$ and 2, respectively. Since the suboptimal strategies

do not require the CSI of the SR and RD links in selecting the best antenna pair, the implementation complexity is less compared with the diversity-optimal strategy at the expense of performance degradation. From the SEP performance comparison, it is observed that S1 achieves better SEP performance compared with S2 and S3 over identical and nonidentical Rayleigh fading channels. However, S1 requires more CSI at D to achieve better SEP performance. Furthermore, S2 outperforms S3 in terms of the SEP performance at the cost of more CSI requirement at D for both identical and nonidentical fading scenarios.

APPENDIX UPPER-BOUND EXPRESSIONS FOR DIVERSITY-OPTIMAL STRATEGY

After simplification, the upper bounds on $A_1(\cdot, \cdot)$ and $A_2(\cdot, \cdot)$ in closed form are given by (81a) and (82a), shown at the top of the page.

REFERENCES

- [1] M. D. Selvaraj and R. K. Mallik, "Error analysis of the decode and forward protocol with selection combining," *IEEE Trans. Wireless Commun.*, vol. 8, no. 6, pp. 3086–3094, Jun. 2009.
- [2] M. R. Bhatnagar and A. Hjørungnes, "ML decoder for decode-and-forward based cooperative communication system," *IEEE Trans. Wireless Commun.*, vol. 10, no. 12, pp. 4080–4090, Dec. 2011.
- [3] M. D. Selvaraj and R. K. Mallik, "Performance of full CSI selection combining for cooperative diversity systems," *IEEE Trans. Commun.*, vol. 60, no. 9, pp. 2482–2488, Sep. 2012.
- [4] M. M. Fareed and M. Uysal, "On relay selection for decode-and-forward relaying," *IEEE Trans. Wireless Commun.*, vol. 8, no. 7, pp. 3341–3346, Jul. 2009.
- [5] T. Q. Duong, V. N. Q. Bao, and H. Zepernick, "On the performance of selection decode-and-forward relay networks over Nakagami- m fading channels," *IEEE Commun. Lett.*, vol. 13, no. 3, pp. 172–174, Mar. 2009.
- [6] D. S. Michalopoulos and G. K. Karagiannidis, "Performance analysis of single relay selection in Rayleigh fading," *IEEE Trans. Wireless Commun.*, vol. 7, no. 10, pp. 3718–3724, Oct. 2008.
- [7] D. S. Michalopoulos and G. K. Karagiannidis, "Two-relay distributed switch and stay combining," *IEEE Trans. Commun.*, vol. 56, no. 11, pp. 1790–1794, Nov. 2008.

- [8] A. M. Salhab and S. A. Zummo, "Performance of switch-and-examine DF relay systems with CCI at the relays and destination over Rayleigh fading channels," *IEEE Trans. Veh. Technol.*, vol. 63, no. 6, pp. 2731–2743, Jul. 2014.
- [9] M. R. Bhatnagar and Arti M. K., "Selection beamforming and combining in decode-and-forward MIMO relay networks," *IEEE Commun. Lett.*, vol. 17, no. 8, pp. 1556–1559, Aug. 2013.
- [10] Arti M. K. and M. R. Bhatnagar, "Performance analysis of hop-by-hop beamforming and combining in DF MIMO relay system over Nakagami- m fading channels," *IEEE Commun. Lett.*, vol. 17, no. 11, pp. 2080–2083, Nov. 2013.
- [11] A. Bansal, M. R. Bhatnagar, A. Hjørungnes, and Z. Han, "Low-complexity decoding in DF MIMO relaying system," *IEEE Trans. Veh. Technol.*, vol. 62, no. 3, pp. 1123–1137, Mar. 2013.
- [12] G. Amarasuriya, C. Tellambura, and M. Ardakani, "Performance analysis framework for transmit antenna selection strategies of cooperative MIMO AF relay networks," *IEEE Trans. Veh. Technol.*, vol. 60, no. 7, pp. 3030–3044, Sep. 2011.
- [13] G. Amarasuriya, C. Tellambura, and M. Ardakani, "Joint relay and antenna selection for dual-hop amplify-and-forward MIMO relay networks," *IEEE Trans. Wireless Commun.*, vol. 11, no. 2, pp. 493–499, Feb. 2012.
- [14] M. Ju, H.-K. Song, and I.-M. Kim, "Joint relay-and-antenna selection in multi-antenna relay networks," *IEEE Trans. Commun.*, vol. 58, no. 12, pp. 3417–3422, Dec. 2010.
- [15] X. Jin, J.-S. No, and D.-J. Shin, "Source transmit antenna selection for MIMO decode-and-forward relay networks," *IEEE Trans. Signal Process.*, vol. 61, no. 7, pp. 1657–1662, Apr. 2013.
- [16] V. S. Krishna and M. R. Bhatnagar, "Performance analysis of sub-optimal transmit and receive antenna selection strategies in single relay based DF cooperative MIMO networks," in *Proc. IEEE NCC*, Kanpur, India, 2014, pp. 1–5.
- [17] V. S. Krishna and M. R. Bhatnagar, "A joint antenna and path selection technique in single relay based DF cooperative MIMO networks," *IEEE Trans. Veh. Technol.*, vol. 65, no. 3, pp. 1340–1353, Mar. 2016.
- [18] B. S. Tan, K. H. Li, and K. C. Teh, "Performance study of transmit antenna selection with switch-and-examine combining over Rayleigh fading," *IEEE Trans. Veh. Technol.*, vol. 61, no. 9, pp. 4205–4211, Nov. 2012.
- [19] M. K. Simon and M.-S. Alouini, *Digital Communications Over Fading Channels: A Unified Approach to Performance Analysis*, 2nd ed. Hoboken, NJ, USA: Wiley-Interscience, 2005.
- [20] D. S. Michalopoulos, N. D. Chatzidiamantis, R. Schober, and G. K. Karagiannidis, "The diversity potential of relay selection with practical channel estimation," *IEEE Trans. Wireless Commun.*, vol. 12, no. 2, pp. 481–493, Feb. 2013.
- [21] V. S. Annapureddy, D. V. Marathe, T. R. Ramya, and S. Bhashyam, "Outage probability of Multiple-Input Single-Output (MISO) systems with delayed feedback," *IEEE Trans. Commun.*, vol. 57, no. 2, pp. 319–326, Feb. 2009.
- [22] K. Tourki, H.-C. Yang, and M.-S. Alouini, "Error-rate performance analysis of incremental decode-and-forward opportunistic relaying," *IEEE Trans. Veh. Technol.*, vol. 59, no. 6, pp. 1519–1524, Jun. 2011.



Swaminathan R (S'12) received the B.Tech. degree (with distinction) in electronics and communication engineering from the Shanmugha Arts, Science, Technology and Research Academy, Thanjavur, India, in 2009 and the M.E. degree (with a gold medal) in communication systems from the College of Engineering Guindy, Anna University, Chennai, India, in 2011.

From July 2011 to May 2015, he was a Ph.D. Research Scholar with the Department of Electronics and Electrical Communication Engineering, Indian Institute of Technology Kharagpur, Kharagpur, India. Since June 2015, he has been a Postdoctoral Research Associate with the School of Computer Engineering, Nanyang Technological University, Singapore. His current research interests are in the broad area of performance analysis of wireless digital communication systems over fading channels, emphasizing cooperative communication and spatial modulation techniques. Moreover, his future research directions include blind parameter estimation of forward error correction codes and interleaver, performance analysis of power line communication, free-space optical communication, full-duplex relaying, and energy harvesting communications.



George K. Karagiannidis (M'96–SM'03–F'14) was born in Pithagorion, Samos Island, Greece. He received the University Diploma and Ph.D. degrees in electrical and computer engineering from the University of Patras, Patras, Greece, in 1987 and 1999, respectively.

From 2000 to 2004, he was a Senior Researcher with the Institute for Space Applications and Remote Sensing, National Observatory of Athens, Athens, Greece. In June 2004, he joined the faculty of the Aristotle University of Thessaloniki, Thessaloniki, Greece, where he is currently a Professor with the Department of Electrical and Computer Engineering and the Director of the Digital Telecommunications Systems and Networks Laboratory. He is also Honorary Professor at South West Jiaotong University, Chengdu, China. He is the author or coauthor of more than 400 technical papers published in scientific journals and presented at international conferences. He is also the author of the Greek edition of a book on telecommunications systems and the coauthor of the book *Advanced Optical Wireless Communications Systems* (Cambridge University Press, 2012). His research interests are in the broad area of digital communications systems with emphasis on wireless communications, optical wireless communications, wireless power transfer and applications, molecular communications, communications and robotics, and wireless security.

Dr. Karagiannidis has been involved as a General Chair, a Technical Program Chair, and a member of the Technical Program Committee at several IEEE and non-IEEE conferences. In the past, he was an Editor of the IEEE TRANSACTIONS ON COMMUNICATIONS, a Senior Editor of the IEEE COMMUNICATIONS LETTERS, an Editor of the EURASIP *Journal of Wireless Communications and Networks*, and several times a Guest Editor of the IEEE JOURNAL ON SELECTED AREAS IN COMMUNICATIONS. From 2012 to 2015, he was the Editor-in-Chief of the IEEE COMMUNICATIONS LETTERS. He was also selected as a 2015 Thomson Reuters Highly Cited Researcher.



Rajarshi Roy (M'13) received the B.Eng. degree (with first-class honors) in electronics and telecommunication from Jadavpur University, Kolkata, India, in 1992; the M.Sc. degree in electrical communication engineering from the Indian Institute of Science, Bangalore, India, in 1995; and the Ph.D. degree in electrical engineering with a specialization in networking from Polytechnic University (now known as the New York University Tandon School of Engineering), Brooklyn, NY, USA, in 2001.

In July 2002, he joined the Department of Electronics and Electrical Communication Engineering, Indian Institute of Technology Kharagpur, Kharagpur, India, as an Assistant Professor, where he was later promoted to Associate Professor in 2010. Before this, he was an Analyst Software Engineer with the Performance Analysis Group, Advanced Development Department, Comverse, Wakefield, MA, USA, and an Engineer with the Lucent Technologies India Development Center, Bangalore, India. He was also an Academic Visitor with the Communications Laboratory, Helsinki University of Technology, Espoo, Finland (Fall 2004); a Visiting Scientist with the Applied Statistics Unit of the Indian Statistical Institute, Kolkata (Fall 2001); an Adjunct Teacher with Polytechnic University (Summer 2000); and a summer intern with Bell Laboratories, Holmdel, NJ, USA (Summer 1997). His current research interests include communication networks, network coding, cooperation in communication and control, network science, and control, optimization, resource allocation, and performance evaluation of networked complex systems.